

Z and Z' decays with and without FCNC in 331 models,

A. Carcamo, R. Martínez* and F. Ochoa†
 Departamento de Física, Universidad Nacional,
 Bogotá-Colombia

6th July 2021

Abstract

In the context of the 331 models, we consider constraints on the extra neutral boson Z' predicted by the model, where three different quark family assignments are identified. Using the ansatz of Matsuda as a specific texture for the quark mass matrices, we obtain allowed regions associated with the Z - Z' mixing angle, the mass of the Z' boson and the parameter β which determines different 331 models. The Z_1 and Z_2 decays with and without flavor changing are also considered. The flavor changing decays of the Z_1 boson into quarks at tree level are highly suppressed by the $Z - Z'$ mixing angle, obtaining the same order of magnitude as the standard model prediction at one loop level. The Z_2 decay widths are calculated with and without flavor changing, where oblique radiative corrections at one loop accounts for about 1% – 4% deviations.

1 Introduction

In most of extensions of the standard model (SM), new massive and neutral gauge bosons, called Z' , are predicted. The phenomenological features that arise about such boson have been subject of extensive studies in the literature [1], whose presence is sensitive to experimental observations at low and high energies, and will be of great interest in the next generation of colliders (LHC, ILC) [2]. In particular, it is possible to study some phenomenological features associated with this extra neutral gauge boson through models with gauge symmetry $SU(3)_c \otimes SU(3)_L \otimes U(1)_X$, also called 331 models. These models arise as an interesting alternative to explain the origin of generations [3], where the three families are required in order to cancel chiral anomalies completely [4]. An additional motivation to study these kinds of models comes from the fact that they can also predict the charge quantization for a three family model even when neutrino masses are added [5].

Although cancellation of anomalies leads to some required conditions [6], such criterion alone still permits an infinite number of 331 models. In these models, the electric charge is defined in general as a linear combination of the diagonal generators of the group

$$Q = T_3 + \beta T_8 + XI, \quad (1)$$

*e-mail: remartinezm@unal.edu.co

†e-mail: faochoap@unal.edu.co

where the value of the β parameter determines the fermion assignment and, more specifically, the electric charges of the exotic spectrum. Hence, it is customary to use this quantum number to classify the different 331 models. If we want to avoid exotic charges we are led to only two different models i.e. $\beta = \pm 1/\sqrt{3}$ [6, 7]. An extensive and detailed study of models with β arbitrary has been carried out in ref. [8] for the scalar sector and in ref. [9] for the fermionic and gauge sector.

The group structure of these models leads, along with the SM-neutral boson Z , to the prediction of an additional current associated with a new neutral boson Z' . It is possible to study the low energy deviations of the Z -pole observables through a precision fit of the $Z - Z'$ mixing [10, 11], which may provides indirect constraints on the free parameters of the model (including β). Unlike the Z -boson whose couplings are family independent and the weak interactions at low energy are of universal character, the couplings of Z' are different for the three families due to the $U(1)_X$ values to each of them. In the quark sector each of the 331 families in the weak basis can be assigned in three different ways into mass eigenstates. In this way, in a phenomenological analysis, the allowed region associated with the $Z - Z'$ mixing angle and the physical mass $M_{Z'}$ of the extra neutral boson will depend on the family assignment. This study was carried out in ref. [12] for the two main versions of the 331 models corresponding to $\beta = -\sqrt{3}$ [10] and $\beta = -\frac{1}{\sqrt{3}}$ [7], and in ref. [13] for β arbitrary.

In addition, the study of rare decays provides a framework to evaluate any new physics beyond the SM (for a recent review on the rare Z decays, see ref. [14]). In particular, the SM may induce FCNC in the Z decay by introducing either one loop corrections or effective couplings with dimension 6 [15]. In the SM, the flavor changing processes in the Z gauge sector are forbidden at tree level even though we considered rotations of the fermions from weak to mass eigenstates. In the context of models beyond the SM with extra neutral currents, the $Z - Z'$ mixing produces small deviations that break the universality feature, and induces FCNC at tree level in Z decays [16, 17, 18] when rotations between weak and mass eigenstates are implemented. Such flavor changing couplings are model dependent [19], and its realization could be verified in the future e^+e^- lineal colliders at the TeV scale (TESLA [20]). In the case of 331 models, FCNC at tree level due to the $Z - Z'$ mixing arise only in the quark sector, while the couplings of the leptons with Z and Z' are universal of families (ref. [17] considers new 331 models with FCNC in the lepton sector). We take specific textures for the quark mass matrices in agreement with the current data on the CKM mixing angles. The assignments for texture on mass fermions have been broadly discussed in the literature [21, 22].

In this work we report a phenomenological study of the 331-extra neutral boson. First, we consider indirect limits at the Z resonance for models with β arbitrary, including linear combinations among the quark families. We adopt the texture structure proposed in ref. [21] in order to obtain allowed regions for the $Z - Z'$ mixing angle, the mass of the Z' boson and the values of β for three different assignments of the quark families [23] in mass eigenstates. The above analysis is performed through a χ^2 statistics at 95% CL including correlation data among the observables. Later, we study high energy corrections of the Z' decay in the framework of models with $\beta = 1/\sqrt{3}$. These analysis are performed considering oblique corrections at one loop level, where running coupling constants at $M_{Z'}$ scale are taken into account. We also calculate the FCNC contributions in the Z and Z' decays.

representation	Q_ψ	X_ψ
$q_{m^*L} = \begin{pmatrix} d_{m^*} \\ -u_{m^*} \\ J_{m^*} \end{pmatrix}_L : \mathbf{3}^*$	$\begin{pmatrix} -\frac{1}{3} \\ \frac{2}{3} \\ \frac{1}{6} + \frac{\sqrt{3}\beta}{2} \end{pmatrix}$	$X_{q_{m^*}}^L = \frac{1}{6} + \frac{\beta}{2\sqrt{3}}$
$d_{m^*R}; u_{m^*R}; J_{m^*R} : \mathbf{1}$	$-\frac{1}{3}; \frac{2}{3}; \frac{1}{6} + \frac{\sqrt{3}\beta}{2}$	$X_{d_{m^*}, u_{m^*}, J_{m^*}}^R = -\frac{1}{3}, \frac{2}{3}, \frac{1}{6} + \frac{\sqrt{3}\beta}{2}$
$q_{3L} = \begin{pmatrix} u_3 \\ d_3 \\ J_3 \end{pmatrix}_L : \mathbf{3}$	$\begin{pmatrix} \frac{2}{3} \\ -\frac{1}{3} \\ \frac{1}{6} - \frac{\sqrt{3}\beta}{2} \end{pmatrix}$	$X_{q^{(3)}}^L = \frac{1}{6} - \frac{\beta}{2\sqrt{3}}$
$u_{3R}; d_{3R}; J_{3R} : \mathbf{1}$	$\frac{2}{3}; -\frac{1}{3}; \frac{1}{6} - \frac{\sqrt{3}\beta}{2}$	$X_{u_3, d_3, J_3}^R = \frac{2}{3}, -\frac{1}{3}, \frac{1}{6} - \frac{\sqrt{3}\beta}{2}$
$\ell_{jL} = \begin{pmatrix} \nu_j \\ e_j \\ E_j^{-Q_1} \end{pmatrix}_L : \mathbf{3}$	$\begin{pmatrix} 0 \\ -1 \\ -\frac{1}{2} - \frac{\sqrt{3}\beta}{2} \end{pmatrix}$	$X_{\ell_j}^L = -\frac{1}{2} - \frac{\beta}{2\sqrt{3}}$
$e_{jR}; E_{jR}^{-Q_1}$	$-1; -\frac{1}{2} - \frac{\sqrt{3}\beta}{2}$	$X_{e_j, E_j}^R = -1, -\frac{1}{2} - \frac{\sqrt{3}\beta}{2}$

Table 1: Fermionic content for three generations with β arbitrary. We take $m^* = 1, 2$, and $j = 1, 2, 3$

2 The 331 spectrum for β arbitrary

The 331 fermionic structures for three families is shown in table 1 for β arbitrary, where all leptons transform as $(\mathbf{1}, \mathbf{3}, \mathbf{X}_\ell^L)$ and $(\mathbf{1}, \mathbf{1}, \mathbf{X}_{\ell'}^R)$ under $(SU(3)_c, SU(3)_L, U(1)_X)$, with \mathbf{X}_ℓ^L and $\mathbf{X}_{\ell'}^R$ the $U(1)_X$ values associated with the left- and right-handed leptons, respectively; while the quarks transform as $(\mathbf{3}, \mathbf{3}^*, \mathbf{X}_{q_{m^*}}^L)$, $(\mathbf{3}^*, \mathbf{1}, \mathbf{X}_{q'_{m^*}}^R)$ for the first two families, and $(\mathbf{3}, \mathbf{3}, \mathbf{X}_{q_3}^L)$, $(\mathbf{3}^*, \mathbf{1}, \mathbf{X}_{q'_3}^R)$ for the third family, where $\mathbf{X}_{q_{m^*}}^L$, $\mathbf{X}_{q_3}^L$ and $\mathbf{X}_{q'_{m^*}}^R$, $\mathbf{X}_{q'_3}^R$ correspond to the $U(1)_X$ values for left- and right-handed quarks. We denote $\mathbf{X}_{q_3}^L$ and $\mathbf{X}_{q_{m^*}}^L$ as the values associated with the $SU(3)_L$ space under $\mathbf{3}$ and $\mathbf{3}^*$ representations, respectively. The quantum numbers \mathbf{X}_ψ for each representation are given in the third column from table 1, where the definition of the electric charge in Eq. 1 has been used, demanding charges of $2/3$ and $-1/3$ to the up- and down-type quarks, respectively, and charges of $-1, 0$ for the charged and neutral leptons. We recognize three different possibilities to assign the physical quarks in each family representation as shown in table 2. At low energy, the three models from table 2 are equivalent and there is not any phenomenological feature that allows us to detect differences between them. In fact, they must reduce to the SM which is an universal family model in $SU(2)_L$. However, through the couplings of the three families to the additional neutral current (Z') and the introduction of a mixing angle between Z and Z' , it is possible to recognize differences among the three models at the electroweak scale.

For the scalar sector described by Table 3, we introduce the triplet field χ with vacuum

Representation A	Representation B	Representation C
$q_{mL} = \begin{pmatrix} d, s \\ -u, -c \\ J_1, J_2 \end{pmatrix}_L : \mathbf{3}^*$ $q_{3L} = \begin{pmatrix} t \\ b \\ J_3 \end{pmatrix}_L : \mathbf{3}$	$q_{mL} = \begin{pmatrix} d, b \\ -u, -t \\ J_1, J_3 \end{pmatrix}_L : \mathbf{3}^*$ $q_{3L} = \begin{pmatrix} c \\ s \\ J_2 \end{pmatrix}_L : \mathbf{3}$	$q_{mL} = \begin{pmatrix} s, b \\ -c, -t \\ J_2, J_3 \end{pmatrix}_L : \mathbf{3}^*$ $q_{3L} = \begin{pmatrix} u \\ d \\ J_1 \end{pmatrix}_L : \mathbf{3}$

Table 2: Three different assignments for the $SU(3)_L$ family representation of quarks

	Q_Φ	X_Φ
$\chi = \begin{pmatrix} \chi_1^{\pm Q_1} \\ \chi_2^{\pm Q_2} \\ \xi_\chi + \nu_\chi \pm i\zeta_\chi \end{pmatrix}$	$\begin{pmatrix} \pm \left(\frac{1}{2} + \frac{\sqrt{3}\beta}{2} \right) \\ \pm \left(-\frac{1}{2} + \frac{\sqrt{3}\beta}{2} \right) \\ 0 \end{pmatrix}$	$\frac{\beta}{\sqrt{3}}$
$\rho = \begin{pmatrix} \rho_1^\pm \\ \xi_\rho + \nu_\rho \pm i\zeta_\rho \\ \rho_3^{\mp Q_2} \end{pmatrix}$	$\begin{pmatrix} \pm 1 \\ 0 \\ \mp \left(-\frac{1}{2} + \frac{\sqrt{3}\beta}{2} \right) \end{pmatrix}$	$\frac{1}{2} - \frac{\beta}{2\sqrt{3}}$
$\eta = \begin{pmatrix} \xi_\eta + \nu_\eta \pm i\zeta_\eta \\ \eta_2^{\mp} \\ \eta_3^{\mp Q_1} \end{pmatrix}$	$\begin{pmatrix} 0 \\ \mp 1 \\ \mp \left(\frac{1}{2} + \frac{\sqrt{3}\beta}{2} \right) \end{pmatrix}$	$-\frac{1}{2} - \frac{\beta}{2\sqrt{3}}$

Table 3: Scalar spectrum that break the 331 symmetry and give masses to the fermions.

expectation value (VEV) $\langle \chi \rangle^T = (0, 0, \nu_\chi)$, which induces masses to the third fermionic components. In the second transition it is necessary to introduce two triplets ρ and η with VEV $\langle \rho \rangle^T = (0, \nu_\rho, 0)$ and $\langle \eta \rangle^T = (\nu_\eta, 0, 0)$ in order to give masses to the quarks of type up and down, respectively.

In the gauge boson spectrum associated with the $SU(3)_L \otimes U(1)_X$ gauge group, we are just interested in the physical neutral sector that corresponds to the photon, Z and Z' , which are written in terms of the electroweak basis for β arbitrary as [9]

$$\begin{aligned}
A_\mu &= S_W W_\mu^3 + C_W \left(\beta T_W W_\mu^8 + \sqrt{1 - \beta^2 T_W^2} B_\mu \right), \\
Z_\mu &= C_W W_\mu^3 - S_W \left(\beta T_W W_\mu^8 + \sqrt{1 - \beta^2 T_W^2} B_\mu \right), \\
Z'_\mu &= -\sqrt{1 - \beta^2 T_W^2} W_\mu^8 + \beta T_W B_\mu,
\end{aligned} \tag{2}$$

where the Weinberg angle is defined as

$$S_W = \sin \theta_W = \frac{g'}{\sqrt{g^2 + (1 + \beta^2) g'^2}}, \quad T_W = \tan \theta_W = \frac{g'}{\sqrt{g^2 + \beta^2 g'^2}} \quad (3)$$

and g, g' correspond to the coupling constants of the $SU(3)_L$ and $U(1)_X$ groups, respectively. Further, a small mixing angle between the two neutral currents Z_μ and Z'_μ appears with the following mass eigenstates [9]

$$\begin{aligned} Z_{1\mu} &= Z_\mu C_\theta + Z'_\mu S_\theta; & Z_{2\mu} &= -Z_\mu S_\theta + Z'_\mu C_\theta; \\ \tan \theta &= \frac{1}{\Lambda + \sqrt{\Lambda^2 + 1}}; & \Lambda &= \frac{-2S_W C_W^2 g'^2 \nu_\chi^2 + \frac{3}{2} S_W T_W^2 g^2 (\nu_\eta^2 + \nu_\rho^2)}{g g' T_W^2 [3\beta S_W^2 (\nu_\eta^2 + \nu_\rho^2) + C_W^2 (\nu_\eta^2 - \nu_\rho^2)]}. \end{aligned} \quad (4)$$

3 Neutral currents

Using the fermionic content from table 1, we obtain the following neutral couplings in weak eigenstates [12]

$$\begin{aligned} \mathcal{L}^{NC} &= \frac{g}{2C_W} \left\{ \sum_{j=1}^3 \overline{Q}_j \gamma_\mu [g_v^{Q_j} - g_a^{Q_j} \gamma_5] Q_j Z^\mu + \overline{\ell}_j \gamma_\mu [g_v^{\ell_j} - g_a^{\ell_j} \gamma_5] \ell_j Z^\mu \right. \\ &\quad + \overline{\ell}_j \gamma_\mu [\tilde{g}_v^{\ell_j} - \tilde{g}_a^{\ell_j} \gamma_5] \ell_j Z^{\mu'} + \sum_{m=1}^2 \overline{q}_{m^*} \gamma_\mu [g_v^{q_m} - \tilde{g}_a^{q_m} \gamma_5] q_{m^*} Z^{\mu'} \\ &\quad \left. + \overline{q}_3 \gamma_\mu [\tilde{g}_v^{q_3} - \tilde{g}_a^{q_3} \gamma_5] q_3 Z^{\mu'} \right\}, \end{aligned} \quad (5)$$

where Q_j with $j = 1, 2, 3$ has been written in a SM-like notation i.e. it refers to triplets of quarks associated with the three generations of quarks (SM does not make a difference in the family representations). The vector and axial vector couplings are shown in Table 4 for each component and for any value of β . The results from Table 4 are in agreement with ref. [17], where we can reproduce the couplings of the charged leptons e_j for models L_1 and L_2 , which correspond in our case to $\beta = 1/\sqrt{3}$ and $\beta = -1/\sqrt{3}$, respectively, and where the coupling constants are related as $\tilde{g}_{v,a} = \frac{\mp S_W}{6} C_{v,a}$ for each case. The results are also in agreement with ref. [24] for $\beta = \sqrt{3}, -1/\sqrt{3}$. The vector and axial vector couplings can be written in a short form as

Fermion	g_v^f	g_a^f	\tilde{g}_v^f	\tilde{g}_a^f
ν_j	$\frac{1}{2}$	$\frac{1}{2}$	$\frac{-1+(1-\sqrt{3}\beta)S_W^2}{2\sqrt{3}\sqrt{1-(1+\beta^2)S_W^2}}$	$\frac{-1+(1-\sqrt{3}\beta)S_W^2}{2\sqrt{3}\sqrt{1-(1+\beta^2)S_W^2}}$
e_j	$-\frac{1}{2} + 2S_W^2$	$-\frac{1}{2}$	$\frac{-1+(1-3\sqrt{3}\beta)S_W^2}{2\sqrt{3}\sqrt{1-(1+\beta^2)S_W^2}}$	$\frac{-1+(1+\sqrt{3}\beta)S_W^2}{2\sqrt{3}\sqrt{1-(1+\beta^2)S_W^2}}$
E_j	$2Q_1S_W^2$	0	$\frac{1-(1+2\sqrt{3}\beta Q_1)S_W^2}{\sqrt{3}\sqrt{1-(1+\beta^2)S_W^2}}$	$\frac{1-S_W^2}{\sqrt{3}\sqrt{1-(1+\beta^2)S_W^2}}$
d_{m^*}	$-\frac{1}{2} + \frac{2}{3}S_W^2$	$-\frac{1}{2}$	$\frac{3-(3+\sqrt{3}\beta)S_W^2}{6\sqrt{3}\sqrt{1-(1+\beta^2)S_W^2}}$	$\frac{1-(1-\sqrt{3}\beta)S_W^2}{2\sqrt{3}\sqrt{1-(1+\beta^2)S_W^2}}$
u_{m^*}	$\frac{1}{2} - \frac{4}{3}S_W^2$	$\frac{1}{2}$	$\frac{3-(3-5\sqrt{3}\beta)S_W^2}{6\sqrt{3}\sqrt{1-(1+\beta^2)S_W^2}}$	$\frac{1-(1+\sqrt{3}\beta)S_W^2}{2\sqrt{3}\sqrt{1-(1+\beta^2)S_W^2}}$
J_{m^*}	$-2Q_{J_m}S_W^2$	0	$\frac{-1+(1+2\sqrt{3}\beta Q_{J_m})S_W^2}{\sqrt{3}\sqrt{1-(1+\beta^2)S_W^2}}$	$\frac{-1+S_W^2}{\sqrt{3}\sqrt{1-(1+\beta^2)S_W^2}}$
u_3	$\frac{1}{2} - \frac{4}{3}S_W^2$	$\frac{1}{2}$	$\frac{-3+(3+5\sqrt{3}\beta)S_W^2}{6\sqrt{3}\sqrt{1-(1+\beta^2)S_W^2}}$	$\frac{-1+(1-\sqrt{3}\beta)S_W^2}{2\sqrt{3}\sqrt{1-(1+\beta^2)S_W^2}}$
d_3	$-\frac{1}{2} + \frac{2}{3}S_W^2$	$-\frac{1}{2}$	$\frac{-3+(3-\sqrt{3}\beta)S_W^2}{6\sqrt{3}\sqrt{1-(1+\beta^2)S_W^2}}$	$\frac{-1+(1+\sqrt{3}\beta)S_W^2}{2\sqrt{3}\sqrt{1-(1+\beta^2)S_W^2}}$
J_3	$-2Q_{J_3}S_W^2$	0	$\frac{1-(1-2\sqrt{3}\beta Q_{J_3})S_W^2}{\sqrt{3}\sqrt{1-(1+\beta^2)S_W^2}}$	$\frac{1-S_W^2}{\sqrt{3}\sqrt{1-(1+\beta^2)S_W^2}}$

Table 4: Vector and axial vector couplings of fermions and massive neutral bosons (Z, Z').

$$\begin{aligned}
g_v^f &= T_3 - 2Q_f S_W^2, \\
g_a^f &= T_3 \\
\tilde{g}_{v,a}^{qm} &= \frac{g' C_W}{g T_W} \left[T_8 + \beta Q_{q_m} T_W^2 \left(\frac{1}{2} \Lambda_1 \pm 1 \right) \right] \\
\tilde{g}_{v,a}^{q3} &= \frac{g' C_W}{g T_W} \left[-T_8 + \beta Q_{q_3} T_W^2 \left(\frac{1}{2} \Lambda_2 \pm 1 \right) \right] \\
\tilde{g}_{v,a}^{\ell_j} &= \frac{g' C_W}{g T_W} \left[-T_8 - \beta T_W^2 \left(\frac{1}{2} \Lambda_3 \mp Q_{\ell_j} \right) \right], \tag{6}
\end{aligned}$$

where $f = Q_j$, ℓ_j in the first line and Q_f the electric charges. The Gell-Mann matrices $T_3 = \frac{1}{2} \text{diag}(1, -1, 0)$ and $T_8 = \frac{1}{2\sqrt{3}} \text{diag}(1, 1, -2)$ are introduced in the notation. We also define $\Lambda_1 = \text{diag}(-1, \frac{1}{2}, 2)$ and $\Lambda_2 = \text{diag}(\frac{1}{2}, -1, 2)$. Finally, ℓ_j denote the leptonic triplets with $\Lambda_3 = \text{diag}(1, 1, 2Q_1)$ and Q_1 defined as the electric charge of the exotic leptons E_j in table 1.

It is noted that $g_{v,a}^f$ are the same as the SM definitions and $\tilde{g}_{v,a}^f$ are β -dependent couplings of Z'_μ (i.e. model dependent). The couplings of Z and all the couplings of leptons are equal for $j = 1, 2, 3$, so that these terms are universal and independent from the representations of table 2. On the other hand, the couplings of the additional gauge boson (Z'_μ) with the two former families are different from the ones involving the third family. This is because the third family transforms differently as remarked in table 1. Consequently, these terms depend from the representation A, B or C .

The Lagrangian can be turned to a weak basis $U^0 = (u^0, c^0, t^0)^T$, $D^0 = (d^0, s^0, b^0)^T$, $N^0 = (\nu_e^0, \nu_\mu^0, \nu_\tau^0)^T$, $E^0 = (e^0, \mu^0, \tau^0)^T$, where the exotic fermions J_j and E_j have been

omitted. In addition, the neutral couplings can be written in terms of the mixing angle between Z_μ and Z'_μ given by Eq. (4), where $Z_{1\mu}$ is the SM-like neutral boson and $Z_{2\mu}$ the exotic ones. Taking a very small angle, we can do $C_\theta \simeq 1$ so that the Lagrangian from Eq. (5) becomes

$$\begin{aligned} \mathcal{L}^{NC} = & \frac{g}{2C_W} \left\{ \overline{U}^0 \gamma_\mu [G_v^{U(r)} - G_a^{U(r)} \gamma_5] U^0 Z_1^\mu + \overline{D}^0 \gamma_\mu [G_v^{D(r)} - G_a^{D(r)} \gamma_5] D^0 Z_1^\mu \right. \\ & + \overline{N}^0 \gamma_\mu [G_v^N - G_a^N \gamma_5] N^0 Z_1^\mu + \overline{E}^0 \gamma_\mu [G_v^E - G_a^E \gamma_5] E^0 Z_1^\mu \\ & + \overline{U}^0 \gamma_\mu [\tilde{G}_v^{U(r)} - \tilde{G}_a^{U(r)} \gamma_5] U^0 Z_2^\mu + \overline{D}^0 \gamma_\mu [\tilde{G}_v^{D(r)} - \tilde{G}_a^{D(r)} \gamma_5] D^0 Z_2^\mu \\ & \left. + \overline{N}^0 \gamma_\mu [\tilde{G}_v^N - \tilde{G}_a^N \gamma_5] N^0 Z_2^\mu + \overline{E}^0 \gamma_\mu [\tilde{G}_v^E - \tilde{G}_a^E \gamma_5] E^0 Z_2^\mu \right\}, \end{aligned} \quad (7)$$

where the couplings associated with $Z_{1\mu}$ are

$$G_{v,a}^{f(r)} = g_{v,a}^f + \delta g_{v,a}^{f(r)}; \quad \delta g_{v,a}^{f(r)} = \tilde{g}_{v,a}^{f(r)} S_\theta, \quad (8)$$

and the couplings associated with $Z_{2\mu}$ are

$$\tilde{G}_{v,a}^{f(r)} = \tilde{g}_{v,a}^{f(r)} - \delta \tilde{g}_{v,a}^f; \quad \delta \tilde{g}_{v,a}^f = g_{v,a}^f S_\theta, \quad (9)$$

where the label (r) in $\tilde{g}^{U,D(r)}$ refers to any of the realizations $r = (A, B, C)$ from table 2. The β -dependent couplings for leptons from Eq. (6) becomes

$$\tilde{g}_{v,a}^\ell = \frac{g' C_W}{2g T_W} \left[\frac{-1}{\sqrt{3}} - \beta T_W^2 \pm 2Q_\ell \beta T_W^2 \right], \quad (10)$$

while for the quark couplings we get

$$\tilde{g}_{v,a}^{q(r)} = \frac{g' C_W}{2g T_W} K^{(r)\dagger} \left[\begin{pmatrix} \frac{1}{\sqrt{3}} + \frac{\beta T_W^2}{3} & & \\ & \frac{1}{\sqrt{3}} + \frac{\beta T_W^2}{3} & \\ & & -\frac{1}{\sqrt{3}} + \frac{\beta T_W^2}{3} \end{pmatrix} \pm 2Q_q \beta T_W^2 \right] K^{(r)}, \quad (11)$$

with $q = U^0, D^0$, and where we define for each representation from table 2

$$K^{(A)} = I, \quad K^{(B)} = \begin{pmatrix} 1 & 0 & 0 \\ 0 & 0 & 1 \\ 0 & 1 & 0 \end{pmatrix}, \quad K^{(C)} = \begin{pmatrix} 0 & 1 & 0 \\ 0 & 0 & 1 \\ 1 & 0 & 0 \end{pmatrix}. \quad (12)$$

We will consider linear combinations among the three families to obtain couplings in mass eigenstates

$$f^0 = R_f f, \quad (13)$$

where f denotes the fermions in mass eigenstates, f^0 in weak eigenstates and R_f the rotation matrix that diagonalize the Yukawa mass terms. Thus, we can write the Eq. (7) in mass eigenstates as

$$\begin{aligned}
\mathcal{L}^{NC} = & \frac{g}{2C_W} \left\{ [\overline{U}\gamma_\mu (\mathfrak{G}_v^{U(r)} - \mathfrak{G}_a^{U(r)}\gamma_5) U + \overline{D}\gamma_\mu (\mathfrak{G}_v^{D(r)} - \mathfrak{G}_a^{D(r)}\gamma_5) D \right. \\
& + \overline{N}\gamma_\mu (G_v^N - G_a^N\gamma_5) N + \overline{E}\gamma_\mu (G_v^E - G_a^E\gamma_5) E] Z_1^\mu \\
& + [\overline{U}\gamma_\mu (\tilde{\mathfrak{G}}_v^{U(r)} - \tilde{\mathfrak{G}}_a^{U(r)}\gamma_5) U + \overline{D}\gamma_\mu (\tilde{\mathfrak{G}}_v^{D(r)} - \tilde{\mathfrak{G}}_a^{D(r)}\gamma_5) D \\
& \left. + \overline{N}\gamma_\mu (\tilde{G}_v^N - \tilde{G}_a^N\gamma_5) N + \overline{E}\gamma_\mu (\tilde{G}_v^E - \tilde{G}_a^E\gamma_5) E] Z_2^\mu \right\}, \quad (14)
\end{aligned}$$

where the couplings of quarks depend on the rotation matrix. Taking into account the definitions from Eqs. (8) and (9), the vector and axial vectors for Z_1 in Eq. (14) take the form

$$\begin{aligned}
R_\ell^\dagger G_{v,a}^\ell R_\ell &= R_\ell^\dagger (g_{v,a}^\ell + \delta g_{v,a}^\ell) R_\ell = G_{v,a}^\ell I, \\
R_q^\dagger G_{v,a}^{q(r)} R_q &= R_q^\dagger (g_{v,a}^q + \delta g_{v,a}^{q(r)}) R_q = g_{v,a}^q I + \delta \mathfrak{g}_{v,a}^{q(r)} = \mathfrak{G}_{v,a}^{q(r)}, \quad (15)
\end{aligned}$$

while for Z_2

$$\begin{aligned}
R_\ell^\dagger \tilde{G}_{v,a}^\ell R_\ell &= R_\ell^\dagger (\tilde{g}_{v,a}^\ell + \delta \tilde{g}_{v,a}^\ell) R_\ell = \tilde{G}_{v,a}^\ell I, \\
R_q^\dagger \tilde{G}_{v,a}^{q(r)} R_q &= R_q^\dagger (\tilde{g}_{v,a}^{q(r)} + \delta \tilde{g}_{v,a}^{q(r)}) R_q = \tilde{\mathfrak{g}}_{v,a}^{q(r)} + \delta g_{v,a}^q I = \tilde{\mathfrak{G}}_{v,a}^{q(r)}. \quad (16)
\end{aligned}$$

Due to the fact that $g_{v,a}^\ell$ (SM couplings) and $\tilde{g}_{v,a}^\ell$ in Eq. (10) are family independent, the neutral couplings in mass eigenstates of leptons are the same as in weak eigenstates, such as indicated by the first lines in Eqs. (15) and (16). However, we obtain flavor changing couplings in the quark sector due to the family dependence shown by $\tilde{g}_{v,a}^{q(r)}$ in Eq. (11), as indicated in the second lines in Eqs (15) and (16), where

$$\delta \mathfrak{g}_{v,a}^{q(r)} = R_q^\dagger \delta g_{v,a}^{q(r)} R_q = \tilde{\mathfrak{g}}_{v,a}^{q(r)} S_\theta, \quad (17)$$

and

$$\tilde{\mathfrak{g}}_{v,a}^{q(r)} = R_q^\dagger \tilde{g}_{v,a}^{q(r)} R_q. \quad (18)$$

For the calculation, we adopt an ansatz on the texture of the quark mass matrices in agreement with the physical masses and mixing angles. The $SU(3)_L \otimes U(1)_X$ Lagrangian for the Yukawa interaction between quarks is

$$\begin{aligned}
-\mathcal{L}_{Yuk} = & \sum_{m=1}^2 \overline{q_{m^*L}} [\Gamma_\eta^{m^*D} \eta D_R^0 + \Gamma_\rho^{m^*U} \rho U_R^0 + \Gamma_\chi^{m^*J} \chi J_{m^*R}^0] \\
& + \overline{q_{3L}} [\Gamma_\rho^{3D} \rho D_R^0 + \Gamma_\eta^{3U} \eta U_R^0 + \Gamma_\chi^{3J} \chi J_{3R}^0] + h.c., \quad (19)
\end{aligned}$$

with η, ρ and χ the scalar triplets from Table 3 and Γ_ϕ^{iQ} being the Yukawa interaction matrices. Taking into account only the $SU(2)_L$ subdoublets (which lie in the two upper

components of the triplet), and omitting the couplings of χ , the mass eigenstates of the scalar sector can be written as [9]

$$\begin{aligned} H &= \begin{pmatrix} \phi_1^\mp \\ h_3^0 + \nu \mp i\phi_3^0 \end{pmatrix} = \rho S_\beta - \eta^* C_\beta, \\ \phi &= \begin{pmatrix} h_2^\mp \\ -h_4^0 \mp ih_1^0 \end{pmatrix} = \rho C_\beta + \eta^* S_\beta, \end{aligned} \quad (20)$$

where η^* denotes the conjugate representation of η , $\tan\beta = \nu_\rho/\nu_\eta$ and $\nu = \sqrt{\nu_\rho^2 + \nu_\eta^2}$. Thus, after some algebraic manipulation, the neutral couplings of the Yukawa Lagrangian can be written as

$$\begin{aligned} -\mathcal{L}_{Yuk}^{(0)} &= \left[\overline{D}_L^0 (M_D) D_R^0 + \overline{U}_L^0 (M_U) U_R^0 \right] \left(1 + \frac{h_3^0 \mp i\phi_3^0}{\nu} \right) \\ &+ \left[\overline{D}_L^0 (\Gamma_D) D_R^0 + \overline{U}_L^0 (\Gamma_U) U_R^0 \right] (h_4^0 \pm ih_1^0) + h.c., \end{aligned} \quad (21)$$

where the fermion masses and Yukawa coupling matrices are given by

$$M = \nu (\Gamma_1 C_\beta + \Gamma_2 S_\beta) \quad \text{and} \quad \Gamma = \Gamma_1 S_\beta - \Gamma_2 C_\beta, \quad (22)$$

where $\Gamma_1 = \Gamma_\eta$ and $\Gamma_2 = \Gamma_\rho$. The Lagrangian from Eq. (21) is equivalent to the two-Higgs-doublet model (2HDM) Lagrangian [25], which exhibits FCNC due to the non-diagonal components of Γ . In particular, we take the structure of mass matrix suggested in ref. [22], which is written in the basis (u^0, c^0, t^0) or (d^0, s^0, b^0) as

$$M_q = \begin{pmatrix} 0 & A_q & A_q \\ A_q & B_q & C_q \\ A_q & C_q & B_q \end{pmatrix}. \quad (23)$$

As studied in ref. [21], there are two possible assignments for the texture components that reproduce the physical mixing angles of the CKM matrix, each one associated with up and down quarks. For up-type quarks, $A_U = \sqrt{\frac{m_t m_u}{2}}$, $B_U = (m_t + m_c - m_u)/2$ and $C_U = (m_t - m_c - m_u)/2$; for down-type quarks $A_D = \sqrt{\frac{m_d m_s}{2}}$, $B_D = (m_b + m_s - m_d)/2$ and $C_D = -(m_b - m_s + m_d)/2$. The above ansatz is diagonalized by the following rotation matrices [21]

$$R_D = \begin{pmatrix} c & s & 0 \\ -\frac{s}{\sqrt{2}} & \frac{c}{\sqrt{2}} & -\frac{1}{\sqrt{2}} \\ -\frac{s}{\sqrt{2}} & \frac{c}{\sqrt{2}} & \frac{1}{\sqrt{2}} \end{pmatrix}; \quad R_U = \begin{pmatrix} c' & 0 & s' \\ -\frac{s'}{\sqrt{2}} & -\frac{1}{\sqrt{2}} & \frac{c'}{\sqrt{2}} \\ -\frac{s'}{\sqrt{2}} & \frac{1}{\sqrt{2}} & \frac{c'}{\sqrt{2}} \end{pmatrix}, \quad (24)$$

with

$$\begin{aligned} c &= \sqrt{\frac{m_s}{m_d + m_s}}; & s &= \sqrt{\frac{m_d}{m_d + m_s}}; \\ c' &= \sqrt{\frac{m_t}{m_t + m_u}}; & s' &= \sqrt{\frac{m_u}{m_t + m_u}}. \end{aligned} \quad (25)$$

For the quark masses, we use the running mass at M_{Z_1} scale given by Eq. (55) in the appendix A, which lead us to the following values

$$c = 0.976; \quad s = 0.219; \quad c' = 0.999; \quad s' = 0.00359. \quad (26)$$

4 Constraints on the $Z - Z'$ mixing and Z_2 mass for β arbitrary

The couplings of the $Z_{1\mu}$ bosons in Eq. (14) have the same form as the SM-neutral couplings, where the vector and axial vector couplings $g_{V,A}^{SM}$ are replaced by $\mathfrak{G}_{V,A} = g_{V,A}^{SM}I + \delta\mathfrak{g}_{V,A}$, and the matrices $\delta\mathfrak{g}_{V,A}$ (given by eq. (17)) are corrections due to the small $Z_\mu - Z'_\mu$ mixing angle θ in mass eigenstates. For this reason all the analytical parameters at the Z -pole have the same SM form but with small correction factors given by $\mathfrak{G}_{V,A}$ that depend on the family assignment. In the SM, the partial decay widths of Z_1 into fermions $f\bar{f}$ is described by [26, 27]:

$$\Gamma_f^{SM} = \frac{N_c^f G_f M_{Z_1}^3}{6\sqrt{2}\pi} \rho_f \sqrt{1 - \mu_f^2} \left[\left(1 + \frac{\mu_f^2}{2}\right) (g_v^f)^2 + (1 - \mu_f^2) (g_a^f)^2 \right] R_{QED} R_{QCD}, \quad (27)$$

where $N_c^f = 1, 3$ for leptons and quarks, respectively. $R_{QED} = 1 + \delta_{QED}^f$ and $R_{QCD} = 1 + \frac{1}{2} (N_c^f - 1) \delta_{QCD}^f$ are QED and QCD corrections given by Eq. (57) in appendix B, and $\mu_f^2 = 4m_f^2/M_Z^2$ considers kinematical corrections only important for the b -quark. Universal electroweak corrections sensitive to the top quark mass are taken into account in $\rho_f = 1 + \rho_t$ and in g_V^{SM} which is written in terms of an effective Weinberg angle [26]

$$\overline{S_W}^2 = \left(1 + \frac{\rho_t}{T_W^2}\right) S_W^2, \quad (28)$$

with $\rho_t = 3G_f m_t^2/8\sqrt{2}\pi^2$. Nonuniversal vertex corrections are also taken into account in the $Z_1 \bar{b}b$ vertex with additional one-loop leading terms which leads to $\rho_b = 1 - \frac{1}{3}\rho_t$ and $\overline{S_W}^2 = \left(1 + \frac{\rho_t}{T_W^2} + \frac{2\rho_t}{3}\right) S_W^2$ [26, 27].

Table 14 from appendix A summarizes some observables at the Z resonance, with their experimental values from CERN collider (LEP), SLAC Liner Collider (SLC) and data from atomic parity violation [26], the SM predictions, and the expressions predicted by 331 models. We use $M_{Z_1} = 91.1876 \text{ GeV}$, $S_W^2 = 0.23113$, and for the predicted SM partial decay given by (27), we use the values from Eq. (56) (see appendix A).

The 331 predictions from table 14 in appendix A are expressed for the LEP Z -pole observables in terms of SM values corrected by

$$\begin{aligned}
 \delta_Z &= \frac{\Gamma_u^{SM}}{\Gamma_Z^{SM}}(\delta_u + \delta_c) + \frac{\Gamma_d^{SM}}{\Gamma_Z^{SM}}(\delta_d + \delta_s) + \frac{\Gamma_b^{SM}}{\Gamma_Z^{SM}}\delta_b + 3\frac{\Gamma_\nu^{SM}}{\Gamma_Z^{SM}}\delta_\nu + 3\frac{\Gamma_e^{SM}}{\Gamma_Z^{SM}}\delta_\ell; \\
 \delta_{had} &= R_c^{SM}(\delta_u + \delta_c) + R_b^{SM}\delta_b + \frac{\Gamma_d^{SM}}{\Gamma_{had}^{SM}}(\delta_d + \delta_s); \\
 \delta_\sigma &= \delta_{had} + \delta_\ell - 2\delta_Z; \\
 \delta A_f &= \frac{\delta \mathbf{g}_V^{ff}}{g_V^f} + \frac{\delta \mathbf{g}_A^{ff}}{g_A^f} - \delta_f,
 \end{aligned} \tag{29}$$

where for the light fermions

$$\delta_f = \frac{2g_v^f \delta \mathbf{g}_v^{ff} + 2g_a^f \delta \mathbf{g}_a^{ff}}{(g_v^f)^2 + (g_a^f)^2}, \tag{30}$$

while for the b -quark

$$\delta_b = \frac{(3 - \beta_K^2) g_v^b \delta \mathbf{g}_v^{bb} + 2\beta_K^2 g_a^b \delta \mathbf{g}_a^{bb}}{\left(\frac{3 - \beta_K^2}{2}\right) (g_v^b)^2 + \beta_K^2 (g_a^b)^2}. \tag{31}$$

The notation $\delta \mathbf{g}_{v,a}^{ff}$ refers to the diagonal part of the matrix $\delta \mathbf{g}_{v,a}$ in Eq. (17). The above expressions are evaluated in terms of the effective Weinberg angle from Eq. (28).

The weak charge is written as

$$Q_W = Q_W^{SM} + \Delta Q_W = Q_W^{SM} (1 + \delta Q_W), \tag{32}$$

where $\delta Q_W = \frac{\Delta Q_W}{Q_W^{SM}}$. The deviation ΔQ_W is [28]

$$\Delta Q_W = \left[\left(1 + 4 \frac{S_W^4}{1 - 2S_W^2} \right) Z - N \right] \Delta \rho_M + \Delta Q'_W, \tag{33}$$

and $\Delta Q'_W$ which contains new physics gives

$$\begin{aligned}
 \Delta Q'_W &= -16 \left[(2Z + N) \left(g_A^e \tilde{\mathbf{g}}_v^{uu} + \tilde{g}_a^e g_V^u \right) + (Z + 2N) \left(g_A^e \tilde{\mathbf{g}}_v^{dd} + \tilde{g}_a^e g_V^d \right) \right] S_\theta \\
 &\quad -16 \left[(2Z + N) \tilde{g}_a^e \tilde{\mathbf{g}}_v^{uu} + (Z + 2N) \tilde{g}_a^e \tilde{\mathbf{g}}_v^{dd} \right] \frac{M_{Z_1}^2}{M_{Z_2}^2}.
 \end{aligned} \tag{34}$$

For cesium, and for the first term in (33) we take the value $\left[\left(1 + 4 \frac{S_W^4}{1 - 2S_W^2} \right) Z - N \right] \Delta \rho_M \simeq -0.01$ [24, 28]. With the definitions of the couplings $\tilde{g}_{V,A}^\ell$ in eq. (10) we can see that the new physics contribution given by Eq. (34) is β -dependent, so that the precision measurements are sensitive to the type of 331 model according to the value of β . This dependence will allow us to perform precision adjustments to β . We get the same correction for the spectrums A

and B due to the fact that the weak charge depends mostly on the up-down quarks, and A, B -cases maintain the same representation for this family.

With the expressions for the Z -pole observables and the experimental data shown in table 14, we perform a χ^2 fit for each representation A, B and C at 95% CL, where the free quantities S_θ, M_{Z_2} and β can be constrained at the Z_1 peak. We assume a covariance matrix with elements $V_{ij} = \rho_{ij}\sigma_i\sigma_j$ among the Z -pole observables, ρ the correlation matrix and σ the quadratic root of the experimental and SM errors. The χ^2 statistic with three degrees of freedom (d.o.f) is defined as [26]

$$\chi^2(S_\theta, M_{Z_2}, \beta) = [\mathbf{y} - \mathbf{F}(S_\theta, M_{Z_2}, \beta)]^T V^{-1} [\mathbf{y} - \mathbf{F}(S_\theta, M_{Z_2}, \beta)], \quad (35)$$

where $\mathbf{y} = \{y_i\}$ represent the 22 experimental observables from table 14, and \mathbf{F} the corresponding 331 prediction. Table 15 from appendix A display the symmetrical correlation matrices taken from ref. [29].

At three d.o.f, we get 3-dimensional allowed regions in the $(S_\theta, M_{Z_2}, \beta)$ space, which correspond to $\chi^2 \leq \chi_{\min}^2 + 7.815$, with $\chi_{\min}^2 = 16.98$ for A and B representations and $\chi_{\min}^2 = 19.27$, for C . The plotted regions in Figs. 1-6 correspond to 2-dimensional cuts in the $S_\theta - \beta$ plane at $M_{Z_2} = 1200, 1500, 4000 \text{ GeV}$, and in the $M_{Z_2} - \beta$ plane at $S_\theta = -0.0008, 0.0005, 0.001$. The results are summarized in tables 5 and 6.

First of all, we find the best allowed region in the plane $S_\theta - \beta$ for three different values of M_{Z_2} . The lowest bound of M_{Z_2} that displays an allowed region is about 1200 GeV, which appears only for the C assignment such as Fig. 1 shows. We can see in the figure that models with negative values of β are excluded, including the usual models with $\beta = -\sqrt{3}, -\frac{1}{\sqrt{3}}$. This non-symmetrical behavior in the sign of β is due to the fact that the vector and axial couplings in Eqs. (10) and (11) have a lineal dependence with β , which causes different results according to the sign. Figs. 2 and 3 display broader allowed regions for $M_{Z_2} = 1500$ and 4000 GeV, respectively. Thus, the possible 331-models are highly restricted by low values of M_{Z_2} (including the exclusion of the main versions), but if the energy scale increases, new 331 versions are accessible. The models from literature are suitable for high values of Z_2 -mass. We also see that for small Z_2 -mass, the bounds associated with the mixing angle are very small ($\sim 10^{-4}$).

On the other hand, we obtain the regions in the plane $M_{Z_2} - \beta$ for small values of S_θ . Fig. 4 shows regions for a negative mixing angle ($S_\theta = -0.0008$), where models with $\beta < 0.75$ are favored. It is interesting to note that regions A and B display thin bounds for M_{Z_2} ($1500 \text{ GeV} < M_{Z_2} < 2500 \text{ GeV}$). Figs. 5 and 6 show regions for positive mixing angles. In particular, we can see in fig. 6 that if $S_\theta = 0.001$, the C-family assignment does not display allowed region. Due to the fact that the A and B spectrums present the same weak corrections, the allowed regions coincide in all plots. We also see that the minima values for M_{Z_2} are mostly extended in the positive values of β , although not too far from zero. We emphasize that, although these results admit continuous values of β , under some circumstances is possible to obtain additional restrictions from basic principles that forbid some specific values, as studied in ref. [9].

M_{Z_2} (GeV)	Quarks Rep.	β	$S_\theta (\times 10^{-4})$
1200	Rep. $A - B$	No Region	No Region
	Rep. C	$1.1 \lesssim \beta \lesssim 1.75$	$-3 \leq S_\theta \leq 2$
1500	Rep. $A - B$	$-0.65 \lesssim \beta \lesssim 1.7$	$-8 \leq S_\theta \leq 6$
	Rep. C	$0.35 \lesssim \beta \lesssim 1.8$	$-6 \leq S_\theta \leq 4$
4000	Rep. $A - B$	$-1.75 \lesssim \beta \lesssim 1.8$	$-7 \leq S_\theta \leq 17$
	Rep. C	$-1.4 \lesssim \beta \lesssim 1.8$	$-10 \leq S_\theta \leq 8$

Table 5: Bounds for β and S_θ for three quark representations at 95% CL and three Z_2 -mass

$S_\theta (\times 10^{-4})$	Quarks Rep.	β	M_{Z_2} (GeV)
-8	Rep. $A - B$	$-0.6 \lesssim \beta \lesssim 0.3$	$1500 \lesssim M_{Z_2} \lesssim 2500$
	Rep. C	$-1 \lesssim \beta \lesssim 0.75$	$1500 \lesssim M_{Z_2}$
5	Rep. $A - B$	$-1.6 \lesssim \beta \lesssim 1.4$	$1500 \lesssim M_{Z_2}$
	Rep. C	$-1.2 \lesssim \beta \lesssim 1.5$	$1700 \lesssim M_{Z_2}$
10	Rep. $A - B$	$-1.15 \lesssim \beta \lesssim 0.85$	$1700 \lesssim M_{Z_2}$
	Rep. C	No Region	No Region

Table 6: Bounds for β and M_{Z_2} for three quark representations at 95% CL and three mixing angle S_θ

5 The Z_2 decay for model with $\beta = 1/\sqrt{3}$

Since the oblique corrections are sensitive to heavy particles running into the loop, we consider the one loop corrections to the Z_2 decay, taking into account the exotic quarks J from table 1, where we assume that the exotic spectrum is degenerated, and $m_{J_1} = m_{J_2} = m_{J_3} \gtrsim M_{Z_2}$. In the \overline{MS} scheme, all the infinite parts of the self-energies are subtracted by properly adding divergent counterterms in the Lagrangian, while the finite terms contribute to the corrections. These calculations are shown in the appendix B, from where we get the following decay width

$$\Gamma_{Z_2 \rightarrow \bar{f}f} = \frac{g^2 M_{Z_2} N_c}{48\pi C_W^2} \sqrt{1 - \mu_f'^2} \left[\left(1 + \frac{\mu_f'^2}{2}\right) \left(\tilde{\mathcal{G}}_v^f\right)^2 + (1 - \mu_f'^2) \left(\tilde{\mathcal{G}}_a^f\right)^2 \right] R_{QED} R_{QCD}. \quad (36)$$

where $\mu_f'^2 = 4m_f^2/M_{Z_2}^2$ takes into account kinematical corrections only important for the top quark. The corrections $R_{QED, QCD}$ are calculated at the M_{Z_2} scale. The effective couplings are

$$\tilde{\mathcal{G}}_v^f = \tilde{g}_v^f - \Delta\tilde{g}_v^f; \quad \tilde{\mathcal{G}}_a^f = \tilde{g}_a^f - \Delta\tilde{g}_a^f, \quad (37)$$

with $\tilde{g}_{v,a}^f$ given by the Eqs. (10) and (11). The effective radiative corrections evaluated at the M_{Z_2} scale are given by

$$\begin{aligned}
\Delta \tilde{g}_v^f &\approx 2S_W C_W Q_f \Pi_{Z_2 \gamma}(M_{Z_2}^2) + g_v^f \Pi_{Z_2 Z_1}(M_{Z_2}^2) \left(1 + \frac{M_{Z_1}^2}{M_{Z_2}^2}\right) + \frac{1}{2} \tilde{g}_v^f \Sigma'_{Z_2 Z_2}(M_{Z_2}^2), \\
\Delta \tilde{g}_a^f &\approx g_a^f \Pi_{Z_2 Z_1}(M_{Z_2}^2) \left(1 + \frac{M_{Z_1}^2}{M_{Z_2}^2}\right) + \frac{1}{2} \tilde{g}_a^f \Sigma'_{Z_2 Z_2}(M_{Z_2}^2).
\end{aligned} \tag{38}$$

Using the definitions from Eqs. (37) and (38), the decay width can be written as (with $(\Delta \tilde{g})^2 \approx 0$)

$$\Gamma_{Z_2 \rightarrow \bar{f} f} = \Gamma_{Z_2 \rightarrow \bar{f} f}^0 (1 - \Delta'_f), \tag{39}$$

where the contribution at tree level is

$$\Gamma_{Z_2 \rightarrow \bar{f} f}^0 = \frac{g^2 M_{Z_2} N_c}{48\pi C_W^2} \sqrt{1 - \mu_f'^2} \left[\left(1 + \frac{\mu_f'^2}{2}\right) (\tilde{g}_v^f)^2 + (1 - \mu_f'^2) (\tilde{g}_a^f)^2 \right] R_{QED} R_{QCD}, \tag{40}$$

and

$$\Delta'_f \approx \frac{2 (\tilde{g}_v^f \Delta \tilde{g}_v^f + \tilde{g}_a^f \Delta \tilde{g}_a^f)}{(\tilde{g}_v^f)^2 + (\tilde{g}_a^f)^2}, \tag{41}$$

that contains the oblique radiative corrections.

We calculate the decay widths taking into account the running coupling constants at the Z_2 resonance. Using the following values at the M_{Z_1} scale

$$\begin{aligned}
\alpha_Y^{-1}(M_{Z_1}) &= 98.36461 \pm 0.06657; & \alpha^{-1}(M_{Z_1}) &= 127.934 \pm 0.027; \\
\alpha_2^{-1}(M_{Z_1}) &= 29.56938 \pm 0.00068; & \alpha_s(M_{Z_1}) &= 0.1187 \pm 0.002; \\
S_W^2(M_{Z_1}) &= 0.23113 \pm 0.00015,
\end{aligned} \tag{42}$$

we get at the $M_{Z_2} \approx 1500$ GeV scale (see appendix C)

$$\begin{aligned}
\alpha_Y^{-1}(M_{Z_2}) &= 95.0867; & \alpha^{-1}(M_{Z_2}) &= 125.993; \\
\alpha_2^{-1}(M_{Z_2}) &= 30.9060; & \alpha_s(M_{Z_2}) &= 0.0853; \\
S_W^2(M_{Z_2}) &= 0.2453,
\end{aligned} \tag{43}$$

while for the quark masses at $M_{Z_2} \approx 1500$ GeV, we get

$$\begin{aligned}
\overline{m}_u(M_{Z_2}) &= 0.00179 \text{ GeV}; & \overline{m}_c(M_{Z_2}) &= 0.537 \text{ GeV}, \\
\overline{m}_t(M_{Z_2}) &= 150.73 \text{ GeV}; & \overline{m}_d(M_{Z_2}) &= 0.00359 \text{ GeV}; \\
\overline{m}_s(M_{Z_2}) &= 0.0717 \text{ GeV}; & \overline{m}_b(M_{Z_2}) &= 2.45 \text{ GeV}.
\end{aligned} \tag{44}$$

	Γ_{ff}^0 (GeV)			Γ_{ff} (GeV)			$\frac{\Gamma^0 - \Gamma}{\Gamma^0} \times 100$ (%)		
	A	B	C	A	B	C	A	B	C
$u\bar{u}$	3.304	3.304	2.293	3.341	3.341	2.317	1.12	1.12	1.05
$c\bar{c}$	3.304	2.293	3.304	3.341	2.317	3.341	1.12	1.05	1.12
$t\bar{t}$	2.170	3.271	3.271	2.193	3.307	3.307	1.06	1.1	1.1
$d\bar{d}$	2.974	2.974	1.963	3.006	3.006	1.982	1.07	1.07	0.97
$s\bar{s}$	2.974	1.963	2.974	3.006	1.982	3.006	1.07	0.97	1.07
$b\bar{b}$	1.963	2.974	2.974	1.982	3.006	3.006	0.97	1.07	1.07
$\ell^+\ell^-$	1.650			1.670			1.21		
$\nu\bar{\nu}$	1.327			1.342			1.13		

Table 7: Partial width of Z_2 into fermions for each representation $A, B,$ and C . Leptons are universal of family. We compare the relative deviations associated with the oblique radiative corrections.

By comparing the data with radiative corrections to the decay $Z \rightarrow b\bar{b}$ carried out in ref [30], exotic quarks with a mass in the range $1.5 - 4$ TeV is found for the 331-bilepton model. Thus, it is reasonable to estimate $m_{J_j} \approx 2$ TeV. With the above values and for $\beta = 1/\sqrt{3}$, we obtain the widths shown in table 7 at both tree and one-loop level from Eqs. (40) and (39), respectively. In the leptonic sector, values independent on the family representation (universal of family) are obtained in the two final rows in table 7, where the radiative corrections accounts for about $(\Gamma^0 - \Gamma)/\Gamma^0 \approx 1.21$ and 1.13 % deviation for charged and neutral leptons, respectively. In regard to the quark widths, we obtain the family dependent decays shown in the table 7, where relative deviations due to one-loop corrections are also calculated.

From the results in table 7, it is possible to do a rough estimative on the branching ratios. Assuming that only decays to SM particles are allowed, we get $Br(Z_2 \rightarrow q\bar{q}) \sim 0.6$ for quarks, $Br(Z_2 \rightarrow \ell^+\ell^-) \sim 0.2$ for charged leptons, and $Br(Z_2 \rightarrow \nu\bar{\nu}) \sim 0.15$ for neutrinos. Comparing with other models [31], we get similar results in the charged sector, but in the neutrino sector, we obtain a branching about two order of magnitude bigger.

6 Phenomenology on the FCNC

In this section we introduce the flavor changing couplings from Eqs (15)-(18) in order to calculate the Z_1 and Z_2 decay widths. As in the above section, we will take the model $\beta = 1/\sqrt{3}$

$\widetilde{G}_{v,a}^{qq'}$			
	A	B	C
$Z_1 u \bar{c}$	$9.57 \times 10^{-4} S_\theta$	$-9.57 \times 10^{-4} S_\theta$	0
$Z_1 u \bar{t}$	$9.57 \times 10^{-4} S_\theta$	$9.57 \times 10^{-4} S_\theta$	$-19.15 \times 10^{-4} S_\theta$
$Z_1 c \bar{t}$	$-0.267 S_\theta$	$0.267 S_\theta$	0
$Z_1 d \bar{s}$	$0.0569 S_\theta$	$0.0569 S_\theta$	$-0.114 S_\theta$
$Z_1 d \bar{b}$	$0.0583 S_\theta$	$-0.0583 S_\theta$	0
$Z_1 s \bar{b}$	$-0.260 S_\theta$	$0.260 S_\theta$	0

Table 8: Vector and axial couplings of $Z_1 qq'$ vertex for each representation A, B, and C. These results correspond to the model $\beta = 1/\sqrt{3}$, where $-0.0007 \leq S_\theta \leq 0.0005$ for A and B representations, and $-0.0005 \leq S_\theta \leq 0.0001$ for C representation.

6.1 The Z_1 decay with FCNC

The couplings from Eq (14) lead to the following partial width of Z_1 into fermions $f\bar{f}'$

$$\Gamma_{ff'} = \frac{N_c^f G_f M_{Z_1}^3}{6\sqrt{2}\pi} \rho_f \left[\left(\mathfrak{G}_v^{ff'(r)} \right)^2 + \left(\mathfrak{G}_a^{ff'(r)} \right)^2 \right] R_{QED} R_{QCD}, \quad (45)$$

where $\mathfrak{G}_{v,a}^{ff'(r)}$ marks the ff' component of the matrices given in Eq. (15). We can see that leptons contribute only for $\ell = \ell'$, while quarks may exhibit FCNC due to the mixing angle and the non-universal couplings of Z_2 . Using the definitions from Eq. (15) and (17), the FCNC contributions to the widths in Eq. (45) can be written for quarks as

$$\Gamma_{Z_1 \rightarrow qq'} = \frac{3G_f M_{Z_1}^3}{6\sqrt{2}\pi} \rho_q \left[\left(\widetilde{\mathfrak{g}}_v^{qq'(r)} \right)^2 + \left(\widetilde{\mathfrak{g}}_a^{qq'(r)} \right)^2 \right] (S_\theta)^2 R_{QED} R_{QCD}, \quad (46)$$

where ρ_q and $R_{QED, QCD}$ are given by Eq. (27). The above width gives the contribution for processes with FCNC at tree level, where we can see that they are suppressed by the small value $(S_\theta)^2$. Table 8 shows the values of the flavor changing electroweak couplings $Z_1 \bar{q} q'$, where the ansatz from Eq. (24) is implemented. It is noted that the Z_1 decay into the top quark is forbidden by kinematical conditions ($m_t > M_{Z_1}$). However, it is possible to calculate the top quark width into the Z_1 boson and light quarks (u, c), obtaining

$$\Gamma_{t \rightarrow Z_1 q} = \frac{\alpha m_t (1 - X_Z^2)^2 (1 + X_Z^2)}{16 S_W^2 C_W^2 X_Z^2} \left[\left(\widetilde{\mathfrak{g}}_v^{tq(r)} \right)^2 + \left(\widetilde{\mathfrak{g}}_a^{tq(r)} \right)^2 \right] (S_\theta)^2, \quad (47)$$

with $X_Z = M_{Z_1}/m_t$.

Using the same values from section 4 at Z_1 -pole, we obtain the FCNC widths shown in table 9 as a fraction of the quadratic mixing angle value S_θ^2 , and for each representation A, B and C.

First, we note that the decays are highly constrained by the quadratic value of the mixing angle. In particular, we can see from Fig. 2 that, for $\beta = 1/\sqrt{3}$, the bounds for the mixing angle in A-B cases are about $-0.0007 \leq S_\theta \leq 0.0005$, from where the FCNC are suppressed

$\Gamma_{qq'}/S_\theta^2$ (MeV)	A-B	C
$Z_1 \rightarrow uc$	1.917×10^{-3}	0
$Z_1 \rightarrow ds$	6.776	27.103
$Z_1 \rightarrow db$	7.116	0
$Z_1 \rightarrow sb$	141.715	0
Γ_{Zq}/S_θ^2 (MeV)	A-B	C
$t \rightarrow Z_1 u$	4.043×10^{-3}	16.172×10^{-3}
$t \rightarrow Z_1 c$	314.081	0

Table 9: Partial width of Z_1 into quarks and top quark into Z_1 -quarks with FCNC for each representation A,B, and C, as a fraction of the quadratic mixing angle value. This results correspond to the model $\beta = 1/\sqrt{3}$, where $-0.0007 \leq S_\theta \leq 0.0005$ for A and B representations, and $-0.0005 \leq S_\theta \leq 0.0001$ for C representation.

by the maximum factor $S_\theta^2 = 4.9 \times 10^{-7}$. Thus, the maxima contributions to the decays $Z_1 \rightarrow uc$ and $t \rightarrow Z_1 u$ are of the order of $10^{-9} - 10^{-10}$ MeV, while for the decays $Z_1 \rightarrow sb$ and $t \rightarrow Z_1 c$ are about 10^{-4} MeV. In particular, we get for the top decay the branching $Br(t \rightarrow Z_1 c) \approx 10^{-7}$. For A-B representations, the decay of the top-quark into the charm quark (i.e. $t \rightarrow Z_1 c$) is about 10^5 times bigger than into the up quark. The source of this difference comes from the texture structure in Eq. (23) and the rotation matrices in Eq (24). A thorough check of Eq. (18), lead us to the following proportions

$$\begin{aligned}
 \tilde{g}_{v,a}^{ut(A,B)} &\sim s' = \sqrt{\frac{m_u}{m_t + m_u}} = 0.0036, \\
 \tilde{g}_{v,a}^{ct(A,B)} &\sim c' = \sqrt{\frac{m_t}{m_t + m_u}} = 0.999,
 \end{aligned}
 \tag{48}$$

where we take the values from Eq. (55) in appendix A at the M_{Z_1} scale. Since the FCNC contributions depends as the quadratic value of the couplings (see Eq. (46)), we obtain a contribution of $s'^2 \sim 10^{-5}$ and $c'^2 \sim 1$ for the decay into u and c , respectively. A similar result is obtained for the down sector, where the width of Z_1 into $s\bar{b}$ quarks is 10^2 times bigger than into $d\bar{b}(\bar{s})$ quarks. Thus, the hierarchical order found in the decay widths from table 9 arises as the result of the mass hierarchical order $m_{u,d} \ll m_{t,b}$. On the other hand, we see that representation C suppress most of the flavor changing decays, which arises as a result of the family structure exhibited by this representation in table 2 when written in mass eigenstates through the rotation matrices from Eq. (24).

6.2 The Z_2 decay with FCNC

Now, we consider the Lagrangian in mass eigenstates from Eq. (14) in the $S_\theta = 0$ limit, where the corrections $\delta g_{V,A}$ disappear. Thus, the Lagrangian that describes FCNC in Eq.

(14) takes the form

$$\mathcal{L}^{FCNC} = \frac{g}{2C_W} [\bar{U}\gamma_\mu (\tilde{\mathfrak{g}}_v^{U(r)} - \tilde{\mathfrak{g}}_a^{U(r)}\gamma_5) U + \bar{D}\gamma_\mu (\tilde{\mathfrak{g}}_v^{D(r)} - \tilde{\mathfrak{g}}_a^{D(r)}\gamma_5) D] Z_2^\mu, \quad (49)$$

with $\tilde{\mathfrak{g}}_{v,a}$ defined by Eq. (18). We take the definitions of the texture structure from Eqs. (23) and (24), whose components are determined by the values from Eq. (25) but with quark masses given by (44) at M_{Z_2} scale, which leads to

$$c = 0.976; \quad s = 0.218; \quad c' = 0.999; \quad s' = 0.00344. \quad (50)$$

We can see that the above components are very similar to the values in Eq. (26) at the Z_1 scale. The values of the couplings associated with the $Z_2 qq'$ vertices are given in Table 10. The width of Z_2 into different flavors of quarks qq' gives

$$\Gamma_{Z_2 \rightarrow qq'} = \Gamma_{Z_2 \rightarrow qq'}^0 (1 - \Delta'_{qq'}), \quad (51)$$

where the tree-level contribution is

$$\Gamma_{Z_2 \rightarrow qq'}^0 = \frac{g^2 M_{Z_2} N_c}{48\pi C_W^2} \left[\left(\tilde{\mathfrak{g}}_v^{qq'} \right)^2 + \left(\tilde{\mathfrak{g}}_a^{qq'} \right)^2 \right], \quad (52)$$

and the radiative corrections due to the $Z_2 - Z_2$ self-energy are contained in

$$\Delta_{qq'} = \frac{2 (\tilde{g}_v^{qq'} \Delta \tilde{g}_v^{qq'} + \tilde{g}_a^{qq'} \Delta \tilde{g}_a^{qq'})}{\left(\tilde{g}_v^{qq'} \right)^2 + \left(\tilde{g}_a^{qq'} \right)^2}, \quad (53)$$

with

$$\Delta \tilde{g}_{v,a}^{qq'} \approx \frac{1}{2} \tilde{g}_{v,a}^{qq'} \Sigma'_{Z_2 Z_2} (M_{Z_2}^2), \quad (54)$$

where $\Sigma'_{Z_2 Z_2}$ is given by Eq. (60) in Appendix B. We consider running coupling constants evaluated at the M_{Z_2} scale, which are given in Eq. (43). In particular, we take the model with $\beta = 1/\sqrt{3}$, whose extra particles do not present exotic charges, and has the lowest bound $M_{Z_2} \approx 1.5 \text{ TeV}$. For the quarks running into the loop, we take again $m_J \approx 2 \text{ TeV}$ [30]. The results are summarized in table (11).

First of all, we note that these values are almost one order of magnitude bigger than the fractions obtained in table 9 associated with the Z_1 boson decay. This behavior is due to the fact that the FCNC widths as a fraction of the mixing angle S_θ^2 in Eqs. (46) and (47) depends on the factor $(\tilde{\mathfrak{g}}_v)^2 + (\tilde{\mathfrak{g}}_a)^2$, which is the same as the one written in Eq. (52). The differences between both cases come basically from the multiplicative factors; in one case proportional to the Z_1 boson mass $M_{Z_1} = 91.1876 \text{ GeV}$, and in the other case to the Z_2 mass $M_{Z_2} \sim 1500 \text{ GeV}$. In addition, the hierarchical order found in the values from table 11 is a direct consequence from the dependence shown by Eq. (48), where the $u\bar{c}(\bar{t})$ and $d\bar{s}(\bar{b})$ decays are lower in about 10^{-5} and 10^{-2} order of magnitude, respectively.

$\tilde{g}_{v,a}^{qq'}$			
	A	B	C
$Z_2 u \bar{c}$	9.15×10^{-4}	-9.15×10^{-4}	0
$Z_2 u \bar{t}$	9.15×10^{-4}	9.15×10^{-4}	-18.29×10^{-4}
$Z_2 c \bar{t}$	-0.265	0.265	0
$Z_2 d \bar{s}$	0.0566	0.0566	-0.113
$Z_2 d \bar{b}$	0.0580	-0.0580	0
$Z_2 s \bar{b}$	-0.259	0.259	0

Table 10: Vector and axial couplings of $Z_2 qq'$ vertex for each representation A,B, and C. This results correspond to the model $\beta = 1/\sqrt{3}$.

$\Gamma_{qq'}$ (MeV)	A-B	C
$Z_2 \rightarrow u \bar{c}$	0.0272	0
$Z_2 \rightarrow u \bar{t}$	0.0272	0.109
$Z_2 \rightarrow c \bar{t}$	2290.65	0
$Z_2 \rightarrow d \bar{s}$	104.15	416.59
$Z_2 \rightarrow d \bar{b}$	109.37	0
$Z_2 \rightarrow s \bar{b}$	2181.31	0

Table 11: Partial width of Z_2 into quarks with FCNC for each representation A,B, and C. These values correspond to the model $\beta = 1/\sqrt{3}$

7 Conclusions

We found three different assignments of quarks into families in mass eigenstates. Each assignment determines different weak couplings of the quarks to the extra neutral current associated with Z' , which exhibits a small mixing angle with the SM-neutral boson Z . The Lagrangian of the Yukawa interaction is equivalent to the 2HDM, which presents flavor changing neutral currents (FCNC) associated with the couplings of the neutral scalars. In particular we adopt the ansatz shown in Eq (23) proposed in ref. [21]. With this texture on the matrices, we studied the constraints on the $Z - Z'$ mixing and Z_2 mass for β arbitrary, obtaining different allowed regions in the $S_\theta - \beta$ and $M_{Z_2} - \beta$ planes for the LEP parameters at the Z -pole. Through a χ^2 fit at the 95% CL and 3 d.o.f, we found regions in the $S_\theta - \beta$ plane that display a dependence in the family assignment for different values of M_{Z_2} (figs. 1 – 3). For the lowest value $M_{Z_2} = 1200$ GeV, we found that only those 331 models with $1.1 \lesssim \beta \lesssim 1.75$ and quarks families in the C-representation, yield a possible region with small mixing angles ($\sim 10^{-4}$). The possibilities of 331-models grow as M_{Z_2} grows, exhibiting broader regions for the mixing angle. For the $M_{Z_2} - \beta$ plots (figs. 4 – 6), we also found model and family restrictions according to the mixing angle. In this case, the β -bound grows when the mixing angle decreases near zero. This behavior seen in the three figures is in agreement with the results from figs. 1 – 3, where the bounds for β acquire their maxima values around $S_\theta = 0$. The Pleitez and Long models ($\beta = -\sqrt{3}, -\frac{1}{\sqrt{3}}$, respectively) are excluded for low values of M_{Z_2} (< 1500 GeV). In fact, we found that the lowest bounds in the M_{Z_2} value are found in regions with $\beta \gtrsim 0$.

The Z_2 decay at $\sqrt{s} \approx M_{Z_2}$ was also studied, where the $Z - Z'$ mixing is highly suppressed. We take the model $\beta = 1/\sqrt{3}$ for the numerical calculations, which holds a typical bound $M_{Z_2} \approx 1500$ GeV and does not exhibit exotic charges in the spectrum. The decay widths were evaluated for each family representation and taking into account oblique radiative corrections associated with the heaviest quarks $J_{1,2,3}$ from table 1 and considering $M_{Z_2} < m_{J_j} \approx 2000$ GeV. We also considered the running coupling constants at the M_{Z_2} scale, obtaining decay widths with values between 1.34 GeV and 3.34 GeV (see table 7). The tree level contributions were also calculated. The radiative corrections account for about 1% deviations. These radiative corrections are sensitive to the mass m_{J_j} of the quarks running into the loop. For instance, the table 12 shows the loop contributions in the scenery with $m_{J_j} \approx 4000$ GeV [30], where we can see that the radiative corrections account for about 5% deviations.

In regard to the FCNC contributions, we found that the Z_1 flavor changing decays are suppressed by the quadratic value of the mixing angle $S_\theta^2 \approx 10^{-7}$. The decays present an hierarchical order due to the texture structure from Eqs. (23) and (24), such as seen in table 9. In fact, the family structure exhibited by representation C suppress most of the flavor changing processes. We may do an estimative about the branching ratios from table 9. For example, we get a maximum value $Br(Z_1 \rightarrow s\bar{b}) \approx 3 \times 10^{-8}$, which is similar to the prediction from the SM [32] at one loop level.

Similar results are obtained for the Z_2 flavor changing decays in table 11, where the values are about one order of magnitude bigger than the fractions obtained for the Z_1 decays. We also evaluated the FCNC of Z_2 decay in the scenery in which $m_{J_j} \approx 4000$ GeV, obtaining the results given in table 13. We see that the widths are slightly larger (about 3%) than the

Γ_{ff} (GeV)			$\frac{\Gamma^0 - \Gamma}{\Gamma^0} \times 100$ (%)			
	A	B	C	A	B	C
$u\bar{u}$	3.470	3.470	2.404	4.74	4.74	4.57
$c\bar{c}$	3.470	2.404	3.470	4.74	4.57	4.74
$t\bar{t}$	2.283	3.437	3.437	4.53	4.75	4.75
$d\bar{d}$	3.119	3.119	2.054	4.63	4.63	4.37
$s\bar{s}$	3.119	2.054	3.119	4.63	4.37	4.63
$b\bar{b}$	2.054	3.119	3.119	4.37	4.63	4.63
$\ell^+\ell^-$	1.732			4.97		
$\nu\bar{\nu}$	1.391			4.80		

Table 12: Partial width of Z_2 into fermions for each representation A, B, and C in the scenery with $m_{J_j} = 4$ TeV.

$\Gamma_{qq'}$ (MeV)	A-B	C
$Z_2 \rightarrow u\bar{c}$	0.0305	0
$Z_2 \rightarrow u\bar{t}$	0.0305	0.122
$Z_2 \rightarrow c\bar{t}$	2369.60	0
$Z_2 \rightarrow d\bar{s}$	107.84	431.35
$Z_2 \rightarrow d\bar{b}$	113.25	0
$Z_2 \rightarrow s\bar{b}$	2255.37	0

Table 13: Partial width of Z_2 into quarks with FCNC for each representation A, B, and C in the scenery of $m_{J_j} = 4$ TeV.

values given in table 11 for $m_{J_j} \approx 2000$ GeV.

We acknowledge the financial support from COLCIENCIAS and HELEN. R. Martinez thanks C.P. Yuan for his hospitality in Michigan State University where part of this work was done.

Appendix

A The Z_1 -pole parameters

The Z_1 -pole parameters with their experimental values from CERN collider (LEP), SLAC Liner Collider (SLC) and data from atomic parity violation taken from ref. [26], are shown in table 14, with the SM predictions and the expressions predicted by 331 models. The corresponding correlation matrix from ref. [29] is given in table 15. For the quark masses, at Z_1 -pole, we use the following values [33]

Quantity	Experimental Values	Standard Model	331 Model
Γ_Z [GeV]	2.4952 ± 0.0023	2.4972 ± 0.0012	$\Gamma_Z^{SM} (1 + \delta_Z)$
Γ_{had} [GeV]	1.7444 ± 0.0020	1.7435 ± 0.0011	$\Gamma_{had}^{SM} (1 + \delta_{had})$
$\Gamma_{(\ell+\ell^-)}$ MeV	83.984 ± 0.086	84.024 ± 0.025	$\Gamma_{(\ell+\ell^-)}^{SM} (1 + \delta_\ell)$
σ_{had} [nb]	41.541 ± 0.037	41.472 ± 0.009	$\sigma_{had}^{SM} (1 + \delta_\sigma)$
R_e	20.804 ± 0.050	20.750 ± 0.012	$R_e^{SM} (1 + \delta_{had} + \delta_e)$
R_μ	20.785 ± 0.033	20.751 ± 0.012	$R_\mu^{SM} (1 + \delta_{had} + \delta_\mu)$
R_τ	20.764 ± 0.045	20.790 ± 0.018	$R_\tau^{SM} (1 + \delta_{had} + \delta_\tau)$
R_b	0.21638 ± 0.00066	0.21564 ± 0.00014	$R_b^{SM} (1 + \delta_b - \delta_{had})$
R_c	0.1720 ± 0.0030	0.17233 ± 0.00005	$R_c^{SM} (1 + \delta_c - \delta_{had})$
A_e	0.15138 ± 0.00216	0.1472 ± 0.0011	$A_e^{SM} (1 + \delta A_e)$
A_μ	0.142 ± 0.015	0.1472 ± 0.0011	$A_\mu^{SM} (1 + \delta A_\mu)$
A_τ	0.136 ± 0.015	0.1472 ± 0.0011	$A_\tau^{SM} (1 + \delta A_\tau)$
A_b	0.925 ± 0.020	0.9347 ± 0.0001	$A_b^{SM} (1 + \delta A_b)$
A_c	0.670 ± 0.026	0.6678 ± 0.0005	$A_c^{SM} (1 + \delta A_c)$
A_s	0.895 ± 0.091	0.9357 ± 0.0001	$A_s^{SM} (1 + \delta A_s)$
$A_{FB}^{(0,e)}$	0.0145 ± 0.0025	0.01626 ± 0.00025	$A_{FB}^{(0,e)SM} (1 + 2\delta A_e)$
$A_{FB}^{(0,\mu)}$	0.0169 ± 0.0013	0.01626 ± 0.00025	$A_{FB}^{(0,\mu)SM} (1 + \delta A_e + \delta A_\mu)$
$A_{FB}^{(0,\tau)}$	0.0188 ± 0.0017	0.01626 ± 0.00025	$A_{FB}^{(0,\tau)SM} (1 + \delta A_e + \delta A_\tau)$
$A_{FB}^{(0,b)}$	0.0997 ± 0.0016	0.1032 ± 0.0008	$A_{FB}^{(0,b)SM} (1 + \delta A_e + \delta A_b)$
$A_{FB}^{(0,c)}$	0.0706 ± 0.0035	0.0738 ± 0.0006	$A_{FB}^{(0,c)SM} (1 + \delta A_e + \delta A_c)$
$A_{FB}^{(0,s)}$	0.0976 ± 0.0114	0.1033 ± 0.0008	$A_{FB}^{(0,s)SM} (1 + \delta A_e + \delta A_s)$
$Q_W(Cs)$	-72.69 ± 0.48	-73.19 ± 0.03	$Q_W^{SM} (1 + \delta Q_W)$

Table 14: The parameters for experimental values, SM predictions and 331 corrections. The values are taken from ref. [26]

$$\begin{aligned}
m_u(M_{Z_1}) &= 2.33_{-0.45}^{+0.42} \text{ MeV}; & m_c(M_{Z_1}) &= 677_{-61}^{+56} \text{ MeV}, \\
m_t(M_{Z_1}) &= 181 \pm 13 \text{ GeV}; & m_d(M_{Z_1}) &= 4.69_{-0.66}^{+0.60} \text{ MeV}, \\
m_s(M_{Z_1}) &= 93.4_{-13.0}^{+11.8} \text{ MeV}; & m_b(M_{Z_1}) &= 3.00 \pm 0.11 \text{ GeV}.
\end{aligned} \tag{55}$$

For the partial SM partial decay given by Eq. (27), we use the following values taken from ref. [26]

$$\begin{aligned}
\Gamma_u^{SM} &= 0.3004 \pm 0.0002 \text{ GeV}; & \Gamma_d^{SM} &= 0.3832 \pm 0.0002 \text{ GeV}; \\
\Gamma_b^{SM} &= 0.3758 \pm 0.0001 \text{ GeV}; & \Gamma_\nu^{SM} &= 0.16729 \pm 0.00007 \text{ GeV}; \\
\Gamma_e^{SM} &= 0.08403 \pm 0.00004 \text{ GeV}.
\end{aligned} \tag{56}$$

Γ_{had}	Γ_ℓ							
1								
.39	1							
A_e	A_μ	A_τ						
1								
.038	1							
.033	.007	1						
R_b	R_c	A_b	A_c	$A_{FB}^{(0,b)}$	$A_{FB}^{(0,c)}$			
1								
-.18	1							
-.08	.04	1						
.04	-.06	.11	1					
-.10	.04	.06	.01	1				
.07	-.06	-.02	.04	.15	1			
Γ_Z	σ_{had}	R_e	R_μ	R_τ	$A_{FB}^{(0,e)}$	$A_{FB}^{(0,\mu)}$	$A_{FB}^{(0,\tau)}$	
1								
-.297	1							
-.011	.105	1						
.008	.131	.069	1					
.006	.092	.046	.069	1				
.007	.001	-.371	.001	.003	1			
.002	.003	.020	.012	.001	-.024	1		
.001	.002	.013	-.003	.009	-.020	.046	1	

Table 15: *The correlation coefficients for the Z-pole observables*

B Radiative corrections

The Z_1 and Z_2 decay in Eqs. (27) and (36) contains global QED and QCD corrections through the definition of $R_{QED} = 1 + \delta_{QED}^f$ and $R_{QCD} = 1 + \frac{1}{2} (N_c^f - 1) \delta_{QCD}^f$, where [26, 27]

$$\begin{aligned}\delta_{QED}^f &= \frac{3\alpha Q_f^2}{4\pi}; \\ \delta_{QCD}^f &= \frac{\alpha_s}{\pi} + 1.405 \left(\frac{\alpha_s}{\pi}\right)^2 - 12.8 \left(\frac{\alpha_s}{\pi}\right)^3 - \frac{\alpha\alpha_s Q_f^2}{4\pi^2}\end{aligned}\quad (57)$$

with α and α_s the electromagnetic and QCD constants, respectively. The values α and α_s are calculated at the M_{Z_1} scale for the Z_1 decays, and at the M_{Z_2} scale for the Z_2 decays.

We are also considering oblique corrections sensitive to the top quark mass in the Z_1 decay. Here, we show the calculation of the oblique corrections corresponding to the Z_2 decay, which is mostly sensitive to the extra quarks masses $m_{J_{1,2,3}}$. The correction due to the Z_2 self-energy leads to the wavefunction renormalization

$$Z_2 \rightarrow Z_{2R} \approx \left(1 - \frac{1}{2} \Sigma_{Z_2 Z_2}^{(fin)'}(q^2)\right) Z_2, \quad (58)$$

where the finite part of the self-energy gives

$$\begin{aligned}\Sigma_{Z_2 Z_2}^{(fin)}(q^2) &\approx \frac{1}{12\pi^2} \left(\frac{g}{2C_W}\right)^2 \sum_{j=1}^3 \left\{ (\tilde{g}_v^{J_j})^2 \left[-q^2 \ln \frac{m_{J_j}^2}{q^2} - \frac{q^2}{3} \right] \right. \\ &\quad \left. + (\tilde{g}_a^{J_j})^2 \left[(6m_{J_j}^2 - q^2) \ln \frac{m_{J_j}^2}{q^2} - \frac{q^2}{3} \right] \right\},\end{aligned}\quad (59)$$

and

$$\begin{aligned}\Sigma_{Z_2 Z_2}^{(fin)'}(q^2) &= \frac{d\Sigma_{Z_2 Z_2}^{(fin)}}{dq^2} = \frac{1}{12\pi^2} \left(\frac{g}{2C_W}\right)^2 \sum_{j=1}^3 \left\{ (\tilde{g}_v^{J_j})^2 \left(\frac{2}{3} - \ln \frac{m_{J_j}^2}{q^2} \right) \right. \\ &\quad \left. + (\tilde{g}_a^{J_j})^2 \left(\frac{2}{3} - \ln \frac{m_{J_j}^2}{q^2} - \frac{6m_{J_j}^2}{q^2} \right) \right\}.\end{aligned}\quad (60)$$

The $Z_2 - Z_1$ self-energy leads to the following vacuum polarization

$$\begin{aligned}\Pi_{Z_2 Z_1}^{(fin)}(q^2) &\approx \frac{1}{12\pi^2} \left(\frac{g}{2C_W}\right)^2 \sum_{j=1}^3 \left\{ \tilde{g}_v^{J_j} g_v^{J_j} \left[-\ln \frac{m_{J_j}^2}{q^2} - \frac{1}{3} \right] \right. \\ &\quad \left. + \tilde{g}_a^{J_j} g_a^{J_j} \left[\left(\frac{6m_{J_j}^2}{q^2} - 1 \right) \ln \frac{m_{J_j}^2}{q^2} - \frac{1}{3} \right] \right\},\end{aligned}\quad (61)$$

and the Z_2 -photon vacuum polarization is given by

$$\Pi_{Z_2\gamma}^{(fin)}(q^2) \approx \frac{1}{12\pi^2} \frac{g^2 S_W}{2C_W} \sum_{j=1}^3 \left\{ Q_{J_j} \tilde{g}_v^{J_j} \left[-\ln \frac{m_{J_j}^2}{q^2} - \frac{1}{3} \right] \right\}, \quad (62)$$

with Q_{J_j} the electric charge of the virtual J_j quarks given in table 1.

C Running masses and coupling constants

The solution of the renormalization group at the lowest one-loop order gives the running coupling constant for $\widetilde{M} \leq \mu$

$$g_i^{-2}(\widetilde{M}) = g_i^{-2}(\mu) + \frac{b_i}{8\pi^2} \ln \left(\frac{\mu}{\widetilde{M}} \right), \quad (63)$$

for $i = 1, 2, 3$, each one corresponding to the constant coupling of $U(1)_Y$, $SU(2)_L$ and $SU(3)_c$, respectively. Specifically, we use the matching condition for the constant couplings, where the $SU(3)_L$ constant is the same as the $SU(2)_L$ constant, i.e. $g_2 = g$. Running the constants at the scale $\mu = M_{Z_2}$ and taking $\widetilde{M} = M_{Z_1}$, we obtain for g_1 and g_2

$$\begin{aligned} g_Y^2(M_{Z_2}) &= \frac{g_Y^2(M_{Z_1})}{1 - \frac{b_1}{8\pi^2} g_Y^2(M_{Z_1}) \ln \left(\frac{M_{Z_2}}{M_{Z_1}} \right)} \\ g^2(M_{Z_2}) &= \frac{g^2(M_{Z_1})}{1 - \frac{b_2}{8\pi^2} g^2(M_{Z_1}) \ln \left(\frac{M_{Z_2}}{M_{Z_1}} \right)} \end{aligned} \quad (64)$$

with

$$\begin{aligned} b_1 &= \frac{20}{9} N_g + \frac{1}{6} N_H + \frac{1}{3} \sum_{\text{sing}} Y^2 = \frac{22}{3}, \\ b_2 &= \frac{4}{3} N_g + \frac{1}{6} N_H + \frac{22}{3} = -3, \end{aligned} \quad (65)$$

where $N_g = 3$ is the number of fermion families and $N_H = 2$ the number of $SU(2)_L$ scalar doublets. With the above definitions, we can obtain the running Weinberg angle

$$\begin{aligned} S_W^2(M_{Z_2}) &= \frac{g_Y^2(M_{Z_2})}{g^2(M_{Z_2}) + g_Y^2(M_{Z_2})} \\ &= S_W^2(M_{Z_1}) \left[\frac{1 - \frac{b_2}{2\pi} \alpha_2(M_{Z_1}) \ln(M_{Z_2}/M_{Z_1})}{1 - \frac{b_1+b_2}{2\pi} \alpha(M_{Z_1}) \ln(M_{Z_2}/M_{Z_1})} \right]. \end{aligned} \quad (66)$$

In order to calculate the running masses for all quarks, we should use the running QCD constant at the n th quark threshold [33], which is defined as

$$\alpha_s^{(n)}(\mu) = \frac{4\pi}{\beta_0^{(n)} L^{(n)}} \left\{ 1 - \frac{2\beta_1^{(n)} \ln [L^{(n)}]}{(\beta_0^{(n)})^2 L^{(n)}} + \frac{4(\beta_1^{(n)})^2}{(\beta_0^{(n)})^4 (L^{(n)})^2} \right. \\ \left. \times \left[\left(\ln(L^{(n)}) - \frac{1}{2} \right)^2 + \frac{\beta_0^{(n)} \beta_2^{(n)}}{8(\beta_1^{(n)})^2} - \frac{5}{4} \right] \right\}, \quad (67)$$

with $L^{(n)} = \ln \left(\frac{\mu^2}{(\Lambda^{(n)})^2} \right)$, $\beta_0^{(n)} = 11 - \frac{2}{3}n_f$, $\beta_1^{(n)} = 51 - \frac{19}{3}n_f$, $\beta_2^{(n)} = 2857 - \frac{5033}{9}n_f + \frac{325}{27}n_f^2$, and n_f the number of quarks with mass less than μ . The asymptotic scale parameters $\Lambda^{(n)}$ for the energy scale μ at each quark threshold are determined by [34]

$$2\beta_0^{(n-1)} \ln \left(\frac{\Lambda^{(n)}}{\Lambda^{(n-1)}} \right) = (\beta_0^{(n)} - \beta_0^{(n-1)}) L^{(n)} + 2 \left(\frac{\beta_1^{(n)}}{\beta_0^{(n)}} - \frac{\beta_1^{(n-1)}}{\beta_0^{(n-1)}} \right) \ln(L^{(n)}) \\ - \frac{2\beta_1^{(n-1)}}{\beta_0^{(n-1)}} \ln \left(\frac{\beta_0^{(n)}}{\beta_0^{(n-1)}} \right) + \frac{4\beta_1^{(n)}}{(\beta_0^{(n)})^2} \left(\frac{\beta_1^{(n)}}{\beta_0^{(n)}} - \frac{\beta_1^{(n-1)}}{\beta_0^{(n-1)}} \right) \frac{\ln(L^{(n)})}{L^{(n)}} \\ + \frac{1}{\beta_0^{(n)}} \left[\left(\frac{2\beta_1^{(n)}}{\beta_0^{(n)}} \right)^2 - \left(\frac{2\beta_1^{(n-1)}}{\beta_0^{(n-1)}} \right)^2 - \frac{\beta_2^{(n)}}{2\beta_0^{(n)}} + \frac{\beta_2^{(n-1)}}{2\beta_0^{(n-1)}} - \frac{22}{9} \right] \frac{1}{L^{(n)}}, \quad (68)$$

where the starting parameter is $\Lambda^{(5)} = 217_{-23}^{+25}$ MeV [26]. We get for each threshold $\mu = m_q^{(n)}$ (with $n = 3$ for the light quarks u, d, s below 1 GeV; and $n = 4, 5, 6$, each one corresponding to the heavy quarks c, b and t , respectively)

$$\Lambda^{(3)} = 342 \text{ MeV}; \quad \Lambda^{(4)} = 301 \text{ MeV}; \quad \Lambda^{(6)} = 91.7 \text{ MeV}. \quad (69)$$

The running mass for the heavy quarks $q = c, b, t$ at $\mu < \mu^{n+1}$ is

$$\overline{m}_{qn}(\mu) = \frac{R^{(n)}(\mu)}{R^{(n)}(m_q^{pole})} m_q^{pole}, \quad (70)$$

while for the light quarks $q = u, d, s$ is

$$\overline{m}_q(\mu) = \frac{R^{(3)}(\mu)}{R^{(3)}(1 \text{ GeV})} m_q(1 \text{ GeV}), \quad (71)$$

where m_q^{pole} are the pole masses and $m_q(1 \text{ GeV})$ are the masses measured at 1 GeV scale. We use the following values [33]

$$\begin{aligned}
 m_c^{pole} &= 1.26 \pm 0.13 \text{ GeV}, & m_b^{pole} &= 4.26 \pm 0.15 \text{ GeV}, \\
 m_t^{pole} &= 174.3 \pm 5.1 \text{ GeV}, & m_u(1 \text{ GeV}) &= 4.88 \pm 0.57 \text{ MeV}, \\
 m_d(1 \text{ GeV}) &= 9.81 \pm 0.65 \text{ MeV}, & m_s(1 \text{ GeV}) &= 195.4 \pm 12.5 \text{ MeV}.
 \end{aligned} \tag{72}$$

We also use

$$\begin{aligned}
 R^{(n)}(\mu) &= \left(\frac{\beta_0 \alpha_s^{(n)}}{2\pi} \right)^{2\gamma_0/\beta_0} \left\{ 1 + \left[\frac{2\gamma_1}{\beta_0} - \frac{\beta_1 \gamma_0}{\beta_0^2} \right] \frac{\alpha_s^{(n)}}{\pi} \right. \\
 &\quad \left. + \frac{1}{2} \left[\left(\frac{2\gamma_1}{\beta_0} - \frac{\beta_1 \gamma_0}{\beta_0^2} \right)^2 + \frac{2\gamma_2}{\beta_0} - \frac{\beta_1 \gamma_1}{\beta_0^2} - \frac{\beta_2 \gamma_0}{16\beta_0^2} + \frac{\beta_1^2 \gamma_0}{2\beta_0^3} \right] \left(\frac{\alpha_s^{(n)}}{\pi} \right)^2 \right\}, \tag{73}
 \end{aligned}$$

with $\gamma_0 = 2$, $\gamma_1 = \frac{101}{12} - \frac{5}{18}n_f$, and $\gamma_2 = \frac{1}{32} [1249 - (\frac{2216}{27} + \frac{160}{3}\zeta(3))n_f - \frac{140}{81}n_f^2]$. In order to get the running mass at $\mu = M_{Z_2} > \mu^{(6)} = m_t$, it is necessary to use the matching condition [34]

$$\overline{m}_{qn}^{(N)}(\mu) = \overline{m}_{qn}^{(N-1)}(\mu) \left[1 + \frac{1}{12} \left(x_N^2 + \frac{5}{3}x_N + \frac{89}{36} \right) \left(\frac{\alpha_s^{(N)}}{\pi} \right)^2 \right]^{-1}, \tag{74}$$

where $x_N = \ln \left[\left(m_{qN}^{(N)} / \mu \right)^2 \right]$, $N > n$, and $\mu_N \leq \mu \leq \mu_{N+1}$. By iterating the above equation, along with the definitions (70) and (71) at each quark threshold, we obtain the values given by Eq. (44).

References

- [1] For a review see A. Leike, Phys. Rep. **317**, 143 (1999); J. Erler, P. Langacker, T.J. Li, Phys. Rev. **D66**, 015002 (2002); S. Hesselbach, F. Franke, H. Fraas, Eur. Phys. J. **C23**, 149 (2002).
- [2] S. Godfrey in Proc. of the APS/DPF/DPB Summer Study on the Future of Particle Physics (Snowmass 2001), ed. N. Graf, arXiv: hep-ph/0201093 and hep-ph/0201092; Marcela Carena, Alejandro Daleo, Bogdan A. Dobrescu, Tim M.P. Tait, Phys. Rev. **D70**, 093009 (2004); G. Weiglein et. al. LHC/LC Study Group, arXiv: hep-ph/0410364
- [3] P.H. Frampton, P.Q. Hung and M. Sher, arXiv: hep-ph/9903387 v2.
- [4] J.S. Bell, R. Jackiw, Nuovo Cim. **A60** 47 (1969); S.L. Adler, Phys. Rev. **177**, 2426 (1969); D.J. Gross, R. Jackiw, Phys.Rev. **D6** 477 (1972). H. Georgi and S. L. Glashow, Phys. Rev. **D6** 429, (1972); S. Okubo, Phys. Rev. **D16**, 3528 (1977); J. Banks and H. Georgi, Phys. Rev. **14** 1159 (1976).

- [5] C.A.deS. Pires and O.P. Ravinez, Phys. Rev. **D58**, 35008 (1998); C.A.deS. Pires, Phys. Rev. **D60**, 075013 (1999).
- [6] L.A. Sánchez, W.A. Ponce, and R. Martínez, Phys. Rev. **D64**, 075013 (2001); R. Martínez, William A. Ponce, Luis A. Sanchez, Phys. Rev. **D65**, 055013 (2002); W.A. Ponce, J.B. Flórez and L.A. Sánchez, Int. J. Mod. Phys. **A17**, 643 (2002); W.A. Ponce, Y. Giraldo, and L.A. Sánchez, Phys. Rev. **D67**, 075001 (2003).
- [7] R. Foot, H.N. Long and T.A. Tran, Phys. Rev. **D50**, R34 (1994); H.N. Long, Phys. Rev. **D53**, 437 (1996); *ibid*, **D54**, 4691 (1996); H.N. Long, Mod. Phys. Lett. **A13**, 1865 (1998).
- [8] Rodolfo A. Diaz, R. Martinez, F. Ochoa, Phys. Rev. **D69**, 095009 (2004).
- [9] Rodolfo A. Diaz, R. Martinez, F. Ochoa, Phys. Rev. **D72**, 035018 (2005)
- [10] F. Pisano and V. Pleitez, Phys. Rev. **D46**, 410 (1992); P.H. Frampton, Phys. Rev. Lett. **69**, 2889 (1992); R. Foot, O.F. Hernandez, F. Pisano and V. Pleitez, Phys. Rev. **D47**, 4158 (1993); P.H. Frampton, P. Krastev and J.T. Liu, Mod. Phys. Lett. **9A**, 761 (1994); P.H. Frampton et. al. Mod. Phys. Lett. **9A**, 1975 (1994); Nguyen Tuan Anh, Nguyen Anh Ky, Hoang Ngoc Long, Int. J. Mod. Phys. **A16**, 541 (2001); J.C. Montero, C.A.deS. Pires and V. Pleitez, Phys. Rev. **D65** (2002) 095001.
- [11] P.H. Frampton and D. Ng, Phys. Rev. **D45**, 4240 (1992).
- [12] Fredy Ochoa and R. Martinez, Phys. Rev. **D72**, 035010 (2005).
- [13] F. Ochoa and R. Martínez, arXiv: hep-ph/0508082.
- [14] M.A. Perez, G. Tavares-Velazco, J.J. Toscano, Int. J. Mod. Phys. **A19**, 159 (2004)
- [15] Ambar Ghosal, Y. Koide, H. Fusaoka, Phys. Rev. **D64**, 053012 (2001); J.I. Illana, T. Riemann, Phys. Rev **D63**, 053004 (2001); D. Delepine, F. Vissani, Phys. Lett. **B522**, 95-101 (2001); T. Rador, Phys. Rev. **D59**, 095012 (1999).
- [16] Paul Langacker, M. Plumacher, Phys. Rev. **D62**, 013006 (2000); V. Barger, Cheng-Wei Chiang, P. Langacker, Hye-Sung Lee, Phys. Lett. **B580**, 186-196 (2004); S. Fajfer, P. Singer, Phys. Rev. **D65**, 017301 (2002).
- [17] D.L. Anderson and M. Sher, Phys. Rev. **D72**, 095014 (2005).
- [18] M.A. Perez, M.A. Soriano, Phys. Rev. **D46**, 125 (1992).
- [19] J. Kang, P. Langacker, Phys. Rev. **D71**, 035014 (2005).
- [20] R.D. Heuer et. al, DESY 2001-011, ECFA 2001-209, arXiv: hep-ph/0106315.
- [21] K. Matsuda, H. Nishiura, Phys. Rev. **D69**, 053005 (2004)

- [22] Y. Koide, H. Nishiura, K. Matsuda, T. Kikuchi and T. Fukuyama, Phys. Rev. **D66**, 093006 (2002); E. Ma and M. Raidal, Phys. Rev. Lett. **87**, 011802 (2001); C.S. Lam, Phys. Lett. **B507**, 214 (2001); K.R.S. Balaji, W. Grimus and T. Schwetz, Phys. Lett. **B508**, 301 (2001); W. Grimus and L. Lavoura, Acta Phys. Pol. **B32**, 3719 (2001); H. Nishiura, K. Matsuda, T. Kikuchi and T. Fukuyama, Phys. Rev. **D65**, 097301 (2002).
- [23] In this connection see K.T. Mahanthappa and P.K. Mohapatra, Phys. Rev. **D42**, 1732-2400 (1990); Phys. Rev. **D43**, 3093 (1991).
- [24] H.N. Long and L.P. Trung, Phys. Lett. **B502** (2001) 63-68.
- [25] J. Gunion, et. al., The Higgs Hunter's Guide (Addison-Wesley, New York, 1990); S. Glashow and S. Weinberg, Phys. Rev. **D15**, 1958 (1977); D. Atwood, L. Reina and A. Soni, Phys. Rev. Lett. **75**, 3800 (1993); Phys. Rev. **D53**, 1199 (1996); Phys. Rev. **D54**, 3296 (1996); Phys. Rev. **D55**, 3156 (1997); M. Sher and Yao Yuan, Phys. Rev. **D44**, 1461 (1991); T.P. Cheng and M. Sher, Phys. Rev. **D35**, 3490 (1987).
- [26] S. Eidelman et. al. Particle Data Group, Phys. Lett. **B592**, (2004), pp. 120-121.
- [27] J. Bernabeu, A. Pich and A. Santamaria, Nucl. Phys. **B363** (1991) 326; D. Bardin et.al. Electroweak Working Group Report, arXiv: hep-ph/9709229 (1997) 28-32.
- [28] G. Altarelli, R. Casalbouni, S. De Curtis, N. Di Bartolomeo, F. Feruglio and R. Gatto, Phys. Lett. **B 261** (1991) 146;
- [29] S. Schael et. al. arXiv: hep-ph/0509008 (submitted to Physics Reports).
- [30] G.A. González-Sprinberg, R. Martínez and O. Sampayo, Phys. Rev. **D71**, 115003 (2005).
- [31] M.A. Perez, G. Tavares-Velasco and J.J. Toscano, Phys. Rev. **D69**, 115004 (2004)
- [32] A. Axelrod, Nucl. Phys. **B209**, 349 (1982); M. Clements et al., Phys. Rev. **D27**, 570 (1983); G. Mann and T. Riemann, Ann. Phys. (Leipzig) **40**, 334 (1984)
- [33] H. Fusaoka and Y. Koide, Phys. Rev. **D57**, 3986 (1998).
- [34] W. Bernreuther and W. Wetzel, Nucl. Phys. **B197**, 228 (1982); W. Bernreuther, Ann. Phys. **151**, 127 (1983); K.G. Chetyrkin, B.A. Kniehl and M. Steinhauser, Phys. Rev. Lett. **79**, 2184 (1997)

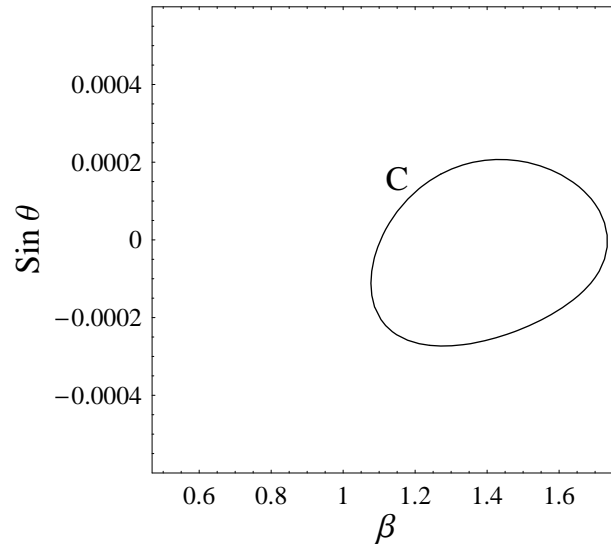


Figure 1: *The allowed region for $\sin \theta$ vs β with $M_{Z_2} = 1200$ GeV. C correspond to the assignment of family from table 2. A and B assignments are excluded at this scale of M_{Z_2} .*

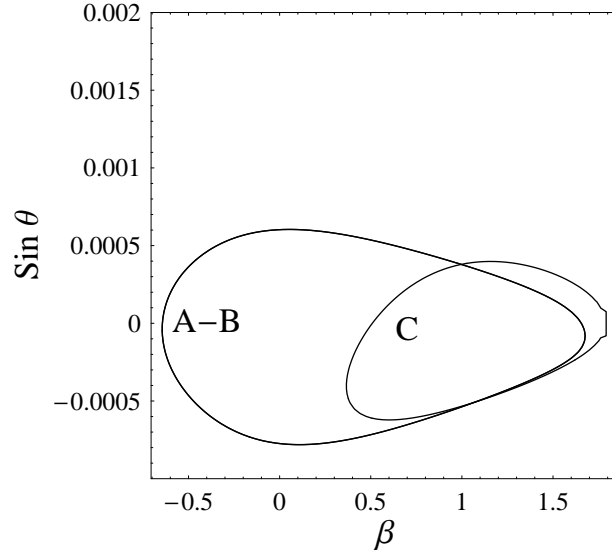


Figure 2: The allowed region for $\sin \theta$ vs β with $M_{Z_2} = 1500$ GeV. A, B and C correspond to the assignment of families from table 2.

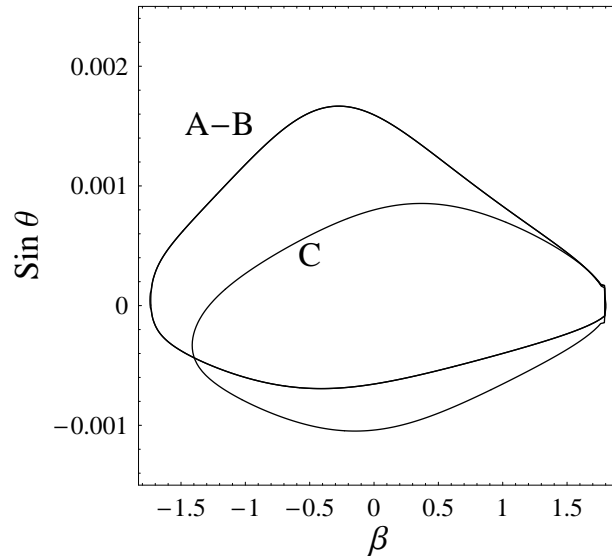


Figure 3: The allowed region for $\sin \theta$ vs β with $M_{Z_2} = 4000$ GeV. A, B and C correspond to the assignment of families from table 2

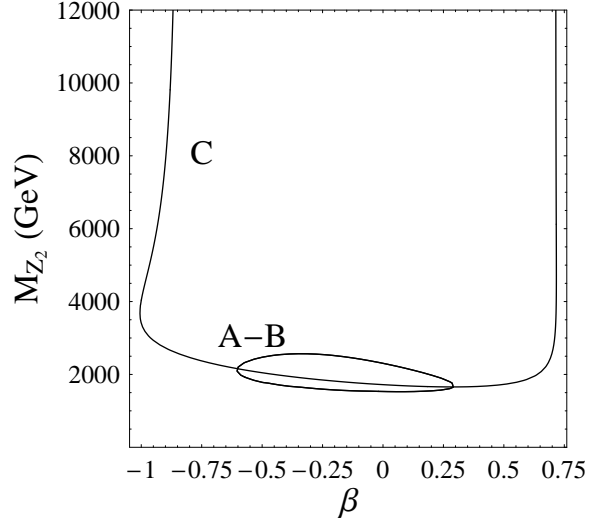


Figure 4: The allowed region for M_{Z_2} vs β with $\sin \theta = -0.0008$. A, B and C correspond to the assignment of families from table 2

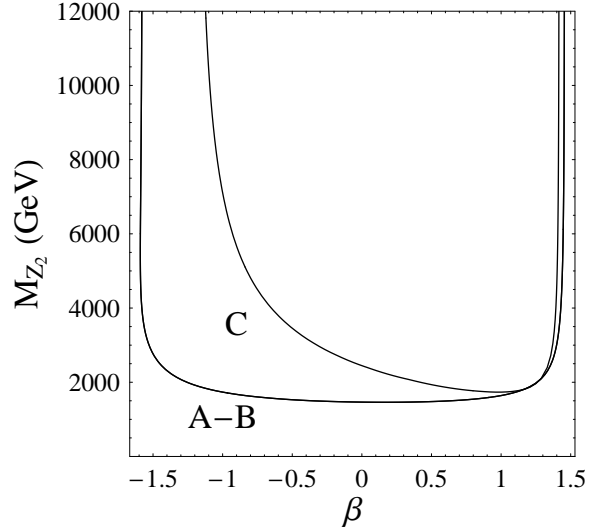


Figure 5: The allowed region for M_{Z_2} vs β with $\sin \theta = 0.0005$. A, B and C correspond to the assignment of families from table 2

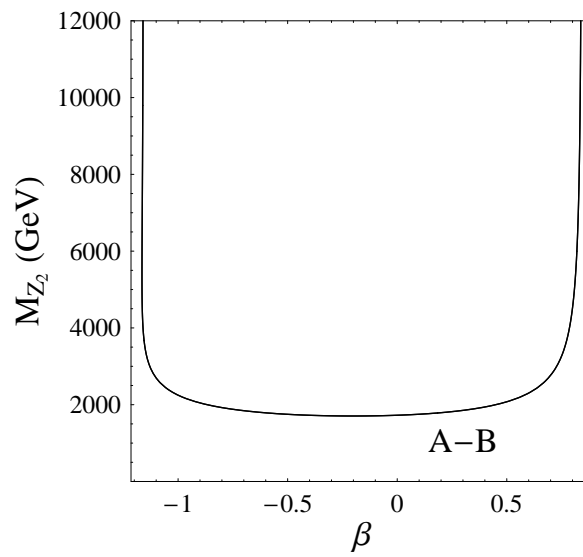


Figure 6: The allowed region for M_{Z_2} vs β with $\sin \theta = 0.001$. A and B correspond to the assignment of families from table 2. The C assignment is excluded for this mixing angle.